Article

Design, Synthesis, and Biological Evaluation of Orally Available First-Generation Dual-Target Selective Inhibitors of Acetylcholinesterase (AChE) and Phosphodiesterase 5 (PDE5) for the Treatment of Alzheimer's Disease

Fei Mao, Huan Wang, Wei Ni, Xinyu Zheng, Manjiong Wang, Keting Bao, Dazheng Ling, Xiaokang Li, Yixiang Xu, Haiyan Zhang, and Jian Li

ACS Chem. Neurosci., **Just Accepted Manuscript** • DOI: 10.1021/acschemneuro.7b00345 • Publication Date (Web): 25 Oct 2017

Design, Synthesis, and Biological Evaluation of Orally Available First-Generation Dual-Target Selective Inhibitors of Acetylcholinesterase (AChE) and Phosphodiesterase 5 (PDE5) for the Treatment of Alzheimer's Disease

Fei Mao[†,#], Huan Wang[‡,§,#], Wei Ni[†,#], Xinyu Zheng[†], Manjiong Wang[†], Keting Bao[†], Dazheng Ling[†], Xiaokang Li[†], Yixiang Xu[†], Haiyan Zhang[‡,⊥,*], Jian Li[†,*]

[†]Shanghai Key Laboratory of New Drug Design, School of Pharmacy, East China University of Science and Technology, 130 Mei Long Road, Shanghai 200237, China

[‡]CAS Key Laboratory of Receptor Research, Shanghai Institute of Materia Medica, Chinese Academy of Sciences, 555 Zu Chong Zhi Road, Shanghai 201203, China

[§]University of Chinese Academy of Science, No.19A Yuquan Road, Beijing 100049, China

[⊥]State Key Laboratory of Drug Research, Shanghai Institute of Materia Medica, University of Chinese Academy of Sciences, Chinese Academy of Sciences, Shanghai 201203, China

[#]These authors contributed equally to this work.

*To whom correspondence should be addressed. jianli@ecust.edu.cn, hzhang@simm.ac.cn

ABSTRACT

Through drug discovery strategies of repurposing and redeveloping existing drugs, a series of novel tadalafil derivatives were rationally designed, synthesized and evaluated to seek dual-target AChE/PDE5 inhibitors as good candidate drugs for AD. Among these derivatives, **1p** and **1w** exhibited excellent selective dual-target AChE/PDE5 inhibitory activities and improved blood-brain barrier (BBB) penetrability. Importantly, **1w·Cit** (citrate of **1w**) could reverse the cognitive dysfunction of scopolamine-induced AD mice and exhibited an excellent effect on enhancing cAMP response element-binding protein (CREB) phosphorylation *in vivo*, a crucial factor in memory formation and synaptic plasticity. Moreover, the molecular docking simulations of **1w** with hAChE and hPDE5A confirmed that our design strategy was rational. In summary, our research provides a potential selective dual-target AChE/PDE5 inhibitor as a good candidate drug for the treatment of AD, and it could also be regarded as a small molecule probe to validate the novel AD therapeutic approach *in vivo*.

KEYWORDS: Alzheimer's disease, Drug repositioning, Dual-target inhibitor, AChE inhibition, PDE5 inhibition

INTRODUCTION

Alzheimer's disease (AD) is a long-term and incurable neuro-degenerative brain disorder clinically characterized by dysmnesia, loss of speech, and behavioral abnormalities.[1] At present, there is no ideal drug for the treatment of AD, and the search for AD drugs remain an urgent issue in the pharmaceutical community. Due to its complex pathogenesis, a single target drug cannot cure this disease fundamentally. Dual or multiple target drugs involved in two or more aspects of AD pathogenesis may generate a synergistic effect and ultimately achieve an ideal therapeutic effect. Thus, the development of multi-target-directed ligands (MTDLs) for the treatment of AD have recently attracted much attention,[2-6] and some studies have confirmed the effectiveness of MTDLs in animal models of dementia,[7-9] supporting the idea that drugs with two or more biological activities may significantly advance the field of anti-AD in the future.

The current anti-AD therapeutic arsenal approved by the United States Food and Drug Administration (FDA) consists of four drugs, donepezil, rivastigmine, galantamine and memantine, which only ameliorate the symptoms of cognitive function but do not cure the disease or reverse its progression. Among them, three are acetylcholinesterase (AChE) inhibitors, and the other, memantine, is an *N*-methyl-D-aspartate receptor (NMDAR) antagonist. In addition, huperzine A (Hup A), which was approved by the Chinese Food and Drug Administration (CFDA) for the treatment of AD, is also an efficient reversible competitive AChE inhibitor. Although inadequate for curing AD, inhibition of AChEs remains the most successful strategy and has been shown to be transiently capable of improving memory and cognitive function in AD patients. Therefore, MTDLs combining AChEs inhibitors with other active pharmacophore within a single drug would generate a more significant reduction in AD symptoms. These compounds not only enhance acetylcholine (ACh) levels in the brain by inhibiting acetylcholinesterase, but also exhibit one or more other anti-AD biological activities such as inhibition of beta amyloid protein (Aβ) production,[10-12] inhibition of Aβ self- or metal-mediated

aggragation,[13-15] monoamine oxidase (MAO) inhibitory activity,[16, 17] serotonergic subtype 4 receptor (5-HT_4R) agonist activity,[18] antioxidation[19] and neuroprotection.[20-22]

Phosphodiesterases (PDEs) comprise a group of enzymes that are responsible for the hydrolysis of cyclic adenosine monophosphate (cAMP) and cyclic guanosine monophosphate (cGMP), which are intracellular second messengers that are closely associated with cellular functions such as neurotransmitter release, neuroplasticity and neuroprotection.[23, 24] Moreover, the elevation of cAMP and/or cGMP levels may promote cAMP response element-binding protein (CREB) phosphorylation, which in turn promotes synaptic plasticity-associated gene transcription and influences long-term memory formation and persistent long-term potentiation (LTP).[25, 26] Ultimately, the increasing levels of cAMP and/or cGMP lead to strengthening of learning and memory ability. Moreover, different PDE inhibitor subtypes have been confirmed to demonstrate significant memory-enhancing effects in animal models,[27-30] especially in models of AD, such as PDE3,[31, 32] PDE4,[33] PDE5,[28, 29] and PDE9,[34] indicating that PDE inhibitors are novel potential therapeutic approaches for the treatment of AD.[35, 36]

PDE5, a special cGMP hydrolytic enzyme, only comprises one hypotype, PDE5A, localized in the hippocampus, cortex and cerebellum of the brain.[37] Research has indicated that the level of cGMP, but not cAMP, is significantly lower in the cerebrospinal fluid (CSF) of mild AD patients compared with non-demented controls, owing to the up-regulation of PDE5 in AD brains.[38] Therefore, PDE5 is a promising therapeutic target in AD, and a PDE5 inhibitor may be a good therapeutic strategy for the treatment of AD patients. Studies have shown that PDE5 inhibitors, such as sildenafil,[39] tadalafil (**1**),[40] and icariin[28] (Figure 1), possess potent anti-AD effects in different mouse models of AD, significantly reversing cognitive impairment and improving learning and memory. In addition, research has indicated that the effects of AChE and PDE5 inhibitors on object recognition memory in rats is different and

dissociable.[41] Therefore, AChE/PDE5 dual inhibitors could play a synergistic anti-AD effect and may supply a new perspective and breakthrough for the treatment of AD.

According to the literature research, no dual-target AChE/PDE5 inhibitor has been reported to date, and hence it is necessary and crucial to search novel dual-target AChE/PDE5 inhibitors to further explore this synergistic therapeutic method. In this study, we will reveal the design, synthesis and biological evaluation of a series of novel, potent, and selective first-generation dual-target AChE/PDE5 inhibitors with good blood-brain barrier (BBB) penetrability and excellent improvement of memory and cognitive function in mice with amnesia, and we anticipated finding a good lead compound for the treatment of AD.

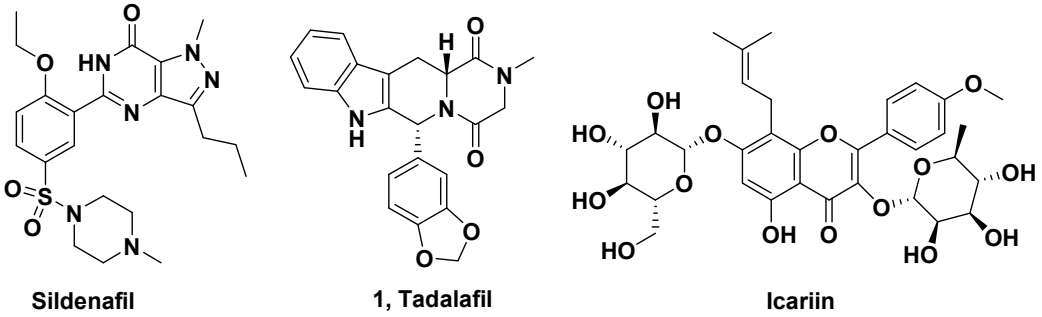

Figure 1. Chemical structures of representative PDE5 inhibitors possessed potent anti-AD effects in mouse models of AD.

DESIGN OF ACHE/PDE5 DUAL INHIBITORS

The drug discovery strategies of new uses for existing drugs have attracted much attention from medicinal chemists and pharmaceutical companies because they are effective, quick and cost-effective.[42] Our group is devoted to research of repurposing and redeveloping existing drugs and has achieved some success.[43-47] Through the screening of our old drug library, tadalafil, a selective PDE5 inhibitor developed by Eli Lilly and approved by the United States FDA for the treatment of erectile dysfunction (ED) in 2003, was found to have certain AChE inhibition (inhibition rate: 65.43% at 40 μM; IC_{50} = 26.159 ± 1.300 μM, Figure 2). In addition, recent studies have shown that tadalafil can reverse cognitive dysfunction in a J20 transgenic mouse

model of AD.[40] Based on the above findings and considering the longer half-life and safety of tadalafil for the chronic treatments of ED and hypertension,[48, 49] it would be an effective compound for the discovery of dual-target AChE/PDE5 inhibitors for the treatment of AD. According to previous structure-activity relationship (SAR) studies of tadalafil analogues,[50, 51] the substituent group at the *N*-atom of piperazine-2,5-dione was replaceable for PDE5 inhibitory activity. In this context, we retained the tadalafil parent nucleus (Figure 2) to maintain PDE5 inhibitory activity, varying only the different substituent group at the *N*-atom of piperazine-2,5-dione, such as morpholine-4-ethyl, 1-benzylpyrrolidine-3-yl, *N*,*N*-dimethylaminoethyl, *N*-methy-*N*-benzylaminoethyl, and substituted or unsubstituted benzylpiperidine (Figure 2, Tables 1-2), expecting to obtain good dual-target AChE/PDE5 inhibitors with improved BBB penetrability and excellent pharmacological activity.

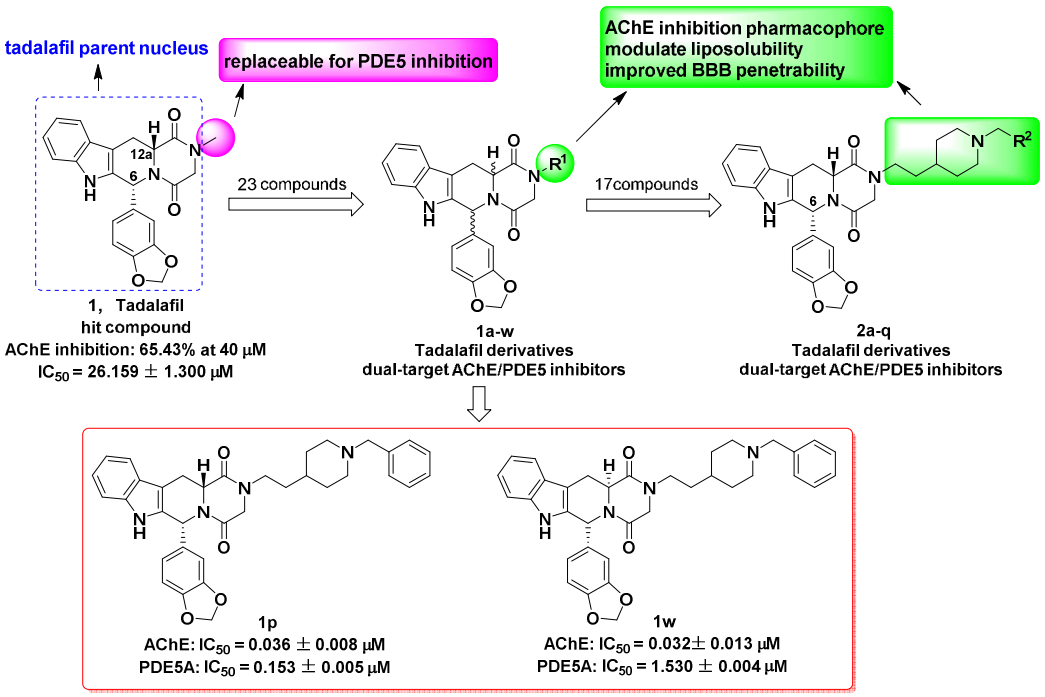

Figure 2. Design strategy for the novel dual-target AChE/PDE5 inhibitors.

CHEMISTRY

The synthetic route for preparation of the key intermediates **3a-d** (two pairs of enantiomers **3a, 3c** and **3b, 3d**) is shown in Scheme 1. The Pictet-Spengler reaction of

commercially available D-tryptophan methyl ester hydrochloride and intermediate **6** (piperonal**)** in isopropanol provided the main cis-intermediate **3a** with a yield of 82%, while it gave an almost equal amount of the cis-intermediate **3a** (38% yield) and trans-intermediate **3b** (40% yield) in ethanol. The Pictet-Spengler reaction of commercially available L-tryptophan methyl ester hydrochloride and intermediate **6** (piperonal**)** in ethanol provided the cis-intermediate **3c** (47% yield) and the trans-intermediate **3d** (32% yield).

Scheme 1. Synthesis of Intermediate **3a-d**[a]

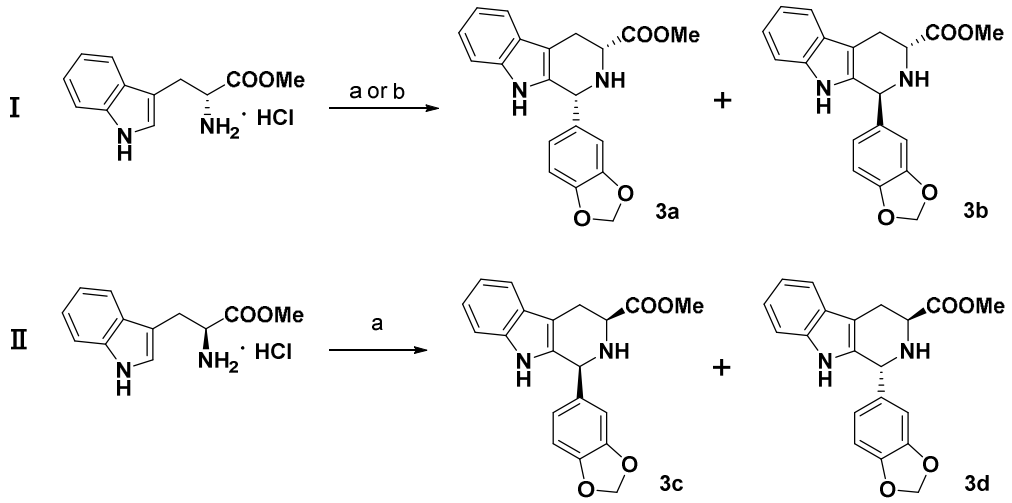

[a]Reagents and conditions: (a) piperonal, EtOH, reflux, 24 h; (b) piperonal, *i*-PrOH, reflux, 24 h.

Scheme 2 depicts the synthetic route of the target compounds **1a-w**. Reaction of **3a-d** with 2-chloroacetyl chloride yielded the key intermediates **4a-d.** In the presence of different primary amines (R^1NH_2, e.g., 2-morpholinoethan-1-amine, 2-(1-benzylpiperidin-4-yl)ethan-1-amine, intermediates **6-13**), the key intermediates **4a-d** proceeded through the cyclization reaction to afford the target compounds **1a-w**.

Scheme 2. Synthesis of Compounds **1a-w**[a]

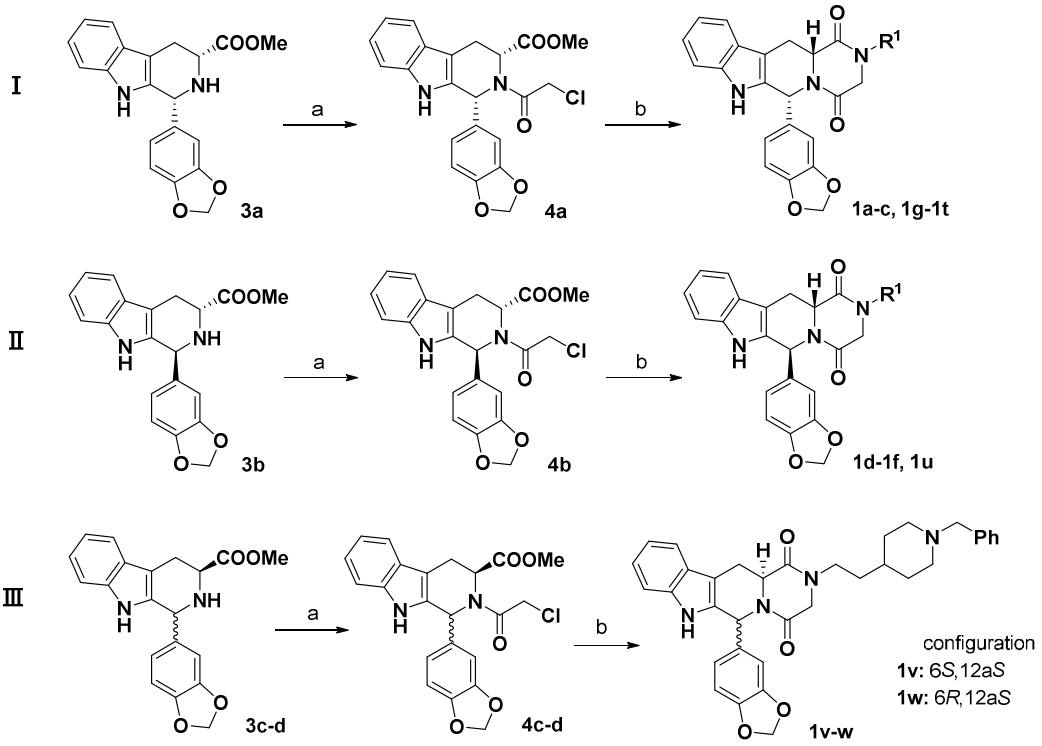

R^1		R^1		R^1	
1a	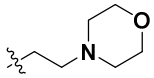	**1h**	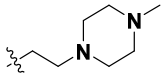	**1o**	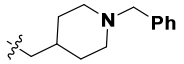
1b	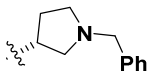	**1i**	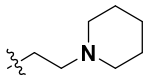	**1p**	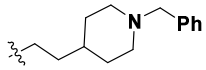
1c	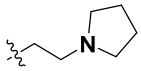	**1j**	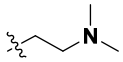	**1q**	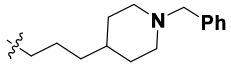
1d	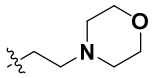	**1k**	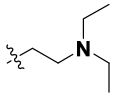	**1r**	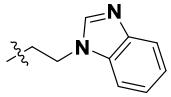
1e	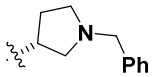	**1l**	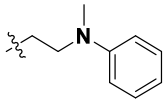	**1s**	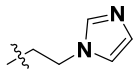
1f	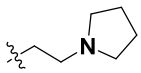	**1m**	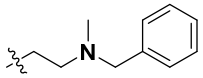	**1t**	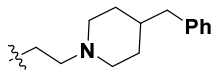
1g	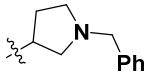	**1n**	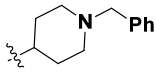	**1u**	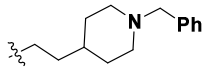

[a]Reagents and conditions: (a) 2-chloroacetyl chloride, Et_3N, DCM, −10 °C to rt, 6 h; (b) R^1NH_2, Et_3N, MeOH, reflux, 12-24 h; (c) 2-(1-benzylpiperidin-4-yl)ethan-1-amine, Et_3N, MeOH, reflux, overnight.

Target compounds **2a-q** were synthesized as illustrated in Scheme 3. Debenzylation of compound **1q** in the presence of 10% Pd/C and H_2 at room temperature and atmospheric pressure gave intermediate **5**, which then reacted with the bromoethane (bromomethyl)cyclohexane, substituted benzyl or bromide benzyl bromide-generated target compounds **2a-q**.

Scheme 3. Synthesis of Compounds **2a-q**[a]

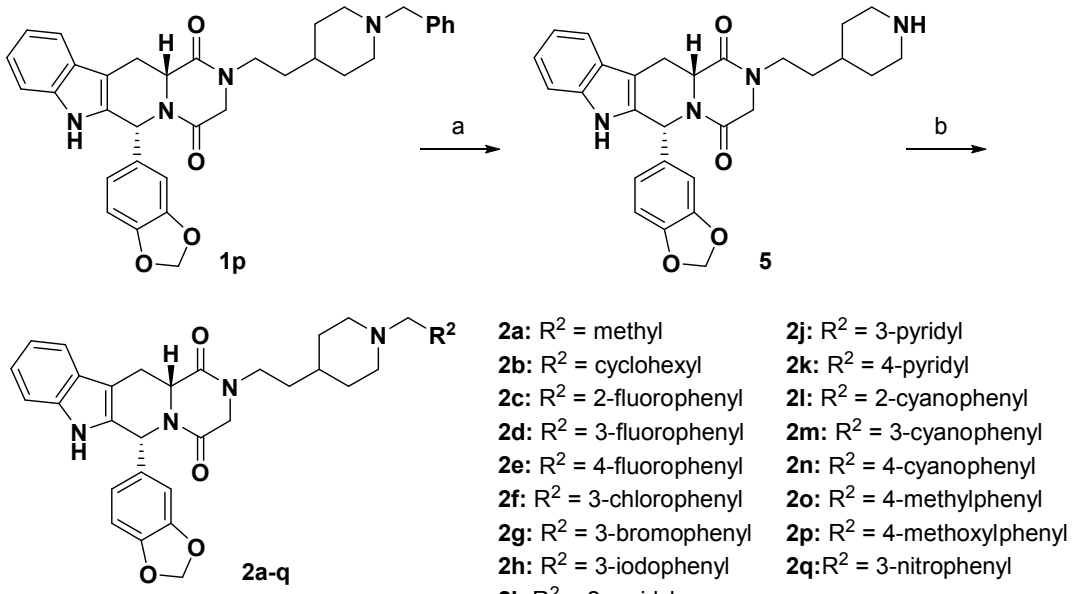

[a]Reagents and conditions: (a) Pd/C, H_2, MeOH, rt, overnight; (b) R^2CH_2Cl or R^2CH_2Br, K_2CO_3, rt, 12-24 h.

The details of the synthetic procedures and structural characterizations of intermediates **3-5** and target compounds **1a-w** and **2a-q** are described in the experimental section, and intermediates **6-13** are shown in the *Supporting Information*. The purities of all target compounds were determined by HPLC (Table S1, *Supporting Information*) and were identified as non-PAINS on the web of http://fafdrugs3.mti.univparis-diderot.fr/, as recommended by the editors from the ACS (American Chemical Society).[52]

RESULTS AND DISCUSSION

ChE Inhibitory Activity

Inhibition of these tadalafil derivatives against AChE and butyrylcholinesterase (BuChE) was determined by the modified Ellman method[53] using Hup A and donepezil as positive references. As shown in Tables 1-3, these compounds displayed poor to excellent AChE inhibitory activities and moderate BuChE inhibitory activities.

Table 1. *In vitro* AChE inhibitory activities of compounds **1a-w**[a].

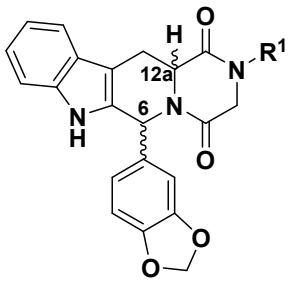

Compd	R^1	Configuration	Inhibition of AChE [I] = 40 μM	IC_{50} ± SD (μM)[b]
1a	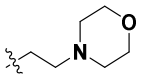	6R,12aR	6.26%	n.t.[c]
1b	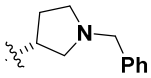	6R,12aR	25.22%	n.t.[c]
1c	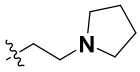	6R,12aR	73.08%	14.206 ± 2.137
1d	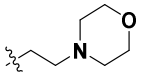	6S,12aR	16.94%	n.t.[c]
1e	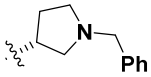	6S,12aR	6.19%	n.t.[c]
1f	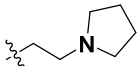	6S,12aR	28.54%	n.t.[c]
1g	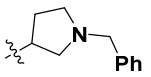	6R,12aR	18.36%	n.t.[c]
1h	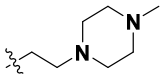	6R,12aR	59.36%	n.t.[c]

1i	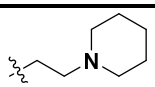	6R,12aR	67.53%	17.529 ± 0.648
1j	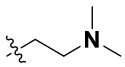	6R,12aR	26.79%	n.t.[c]
1k	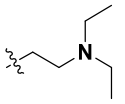	6R,12aR	81.17%	6.728 ± 0.201
1l	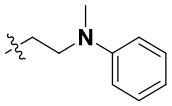	6R,12aR	1.22%	n.t.[c]
1m	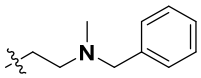	6R,12aR	16.35%	n.t.[c]
1n	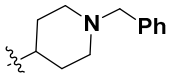	6R,12aR	11.12%	n.t.[c]
1o	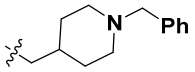	6R,12aR	65.35%	n.t.[c]
1p	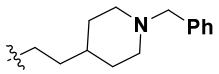	6R,12aR	103.96%	0.036 ± 0.008
1q	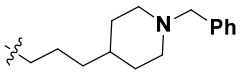	6R,12aR	98.46%	0.075 ± 0.017
1r	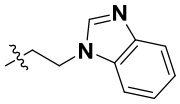	6R,12aR	12.70%	n.t.[c]
1s	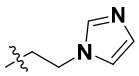	6R,12aR	19.50%	n.t.[c]
1t	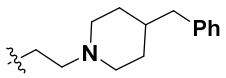	6R,12aR	13.62%	n.t.[c]
1u	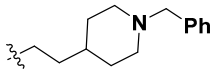	6S,12aR	77.26%	8.140 ± 0.400
1v	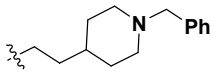	6S,12aS	94.73%	0.851 ± 0.129
1w	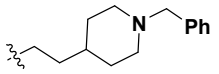	6R,12aS	99.78%	0.032 ± 0.013
Tadalafil	Me	6R,12aR	65.43%	26.159 ± 1.300
Hup A	-	-	-	0.084 ± 0.017

Donepezil	-	-	-	0.013 ± 0.150

[a]AChE from rat cortex. [b]Results are expressed as the mean of at least three experiments. [c]n.t. indicates no test.

Table 2. *In vitro* AChE inhibitory activities of compounds **2a-q**[a].

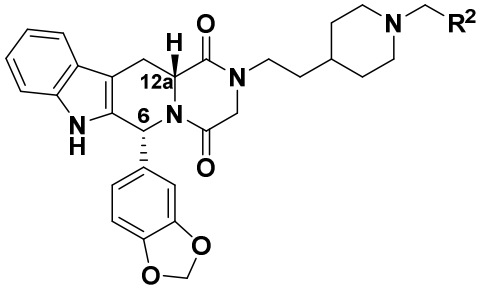

Compd	R^2	Inhibition of AChE ［I］= 40 μM	IC_{50} ± SD (μM)[b]
1p	Ph	103.96%	0.036 ± 0.008
2a	Me	96.31%	1.583 ± 0.216
2b	Cy	101.72%	0.118 ± 0.029
2c	2-fluorophenyl	98.89%	0.067 ± 0.013
2d	3-fluorophenyl	98.34%	0.060 ± 0.014
2e	4-fluorophenyl	101.51%	0.089 ± 0.020
2f	3-chlorophenyl	68.12%	10.440 ± 0.910
2g	3-bromophenyl	64.48%	3.390 ± 0.201
2h	3-iodophenyl	21.60%	n.t.[c]
2i	2-pyridyl	102.67%	0.093 ± 0.008
2j	3-pyridyl	90.03%	0.261 ± 0.030
2k	4-pyridyl	90.93%	0.161 ± 0.016
2l	2-cyanophenyl	25.34%	n.t.[c]
2m	3-cyanophenyl	80.82%	0.800 ± 0.109
2n	4-cyanophenyl	95.73%	0.216 ± 0.045
2o	4-methylphenyl	88.38%	1.689 ± 0.146
2p	4-methoxylphenyl	46.98%	n.t.[c]

2q	3-nitrophenyl	79.41%	0.833 ± 0.061
Tadalafil	-	65.43%	26.159 ± 1.300
Hup A	-	-	0.084 ± 0.017
Donepezil	-	-	0.013 ± 0.150

[a]AChE from rat cortex. [b]Results are expressed as the mean of at least three experiments. [c]n.t. indicates no test.

The R^1 substituent group and absolute configuration remarkably affected the AChE inhibitory activities (Table 1). When R^1 substituent groups changed from methyl (tadalafil) into morpholine-4-ethyl (**1a**), 1-benzylpyrrolidine-3-yl (**1b, 1g**), *N*,*N*-dimethylaminoethyl (**1j**), *N*-methy-*N*-benzylaminoethyl (**1m**), *N*-methyl-*N*-phenylaminoethyl (**1l**), 1*H*-benzo[*d*]imidazole-1-ethyl (**1r**), and 1*H*-imidazole-1-ethyl (**1s**), the AChE inhibitory activities were dramatically decreased, with 1.22-28.54% inhibition at 40 μM. When the R^1 substituent groups changed from methyl (tadalafil) into pyrrolidine-1-ethyl (**1c**), 1-methylpiperazine-4-ethyl (**1h**), piperidine-1-ethyl (**1i**), and *N*,*N*-diethylaminoethyl (**1k**), the AChE inhibitory activities were reserved, with 59.36-81.17% inhibition at 40 μM. Among these tested compounds with an absolute configuration of 6*R*,12a*R*, **1p** with the R^1 substituent group of 1-benzylpiperidine-4-ethyl exhibited the best AChE inhibitory activities, with IC_{50} values of 36 nM. Notably, the chain length between the tadalafil parent nucleus and 1-benzylpiperidine exerted a crucial influence on the AChE inhibitory activities, and the two methylenes between them was the optimal chain length. Directly tethering the 1-benzylpiperidine to the tadalafil parent nucleus led to weak AChE inhibitory activity (**1n**, 11.12% inhibition at 40 μM). Changing the chain length into one methylene (**1o**) or three methylene (**1q**) led to decreased AChE inhibitory activities (**1o,** 65.35% inhibition at 40 μM; **1q**, IC_{50} = 75 nM). Moreover, the substituent pattern of benzylpiperidine also played an important role in AChE inhibition. Reversing the *N* atom position of 1-benzylpiperidine-4-ethyl, which changes the R^1 substituent group 1-benzylpiperidine-4-ethyl (**1p**) into

4-benzylpiperidine-1-ethyl (**1t**), led to a dramatic decline in AChE inhibitory activity (**1t**, 13.62% inhibition at 40 μM).

Furthermore, the influence of stereochemistry on AChE inhibition has been discussed. In the cis-isomers (6*R*,12a*R* and 6*S*,12a*S*), the enantiomer **1p** (6*R*,12a*R*) was the more potent AChE inhibitor (**1p**, IC_{50} = 0.036 μM; **1v**, IC_{50} = 0.815 μM), while in the trans-isomers (6*R*,12a*S* and 6*S*,12a*R*), the enantiomer **1w** (6*R*,12a*S*) was the more potent AChE inhibitor (**1w**, IC_{50} = 0.032 μM; **1u**, IC_{50} = 8.140 μM). The diastereoisomers **1p** and **1w** showed almost the same AChE inhibitory activity, which indicated that the stereo-configuration at position 6 of the tadalafil parent nucleus was key for the strong AChE inhibitory activity.

The influence of the substituent group at the *N*-atom of piperidine (R^2CH_2, Table 2) on AChE inhibitory activities was also studied, and the results are shown in Table 2. Compound **2a** with an ethyl substituent at the *N*-atom of piperidine showed lower AChE inhibition (IC_{50} = 1.583 μM). Compound **2b**, obtained by reducing phenyl to a six-membered nonaromatic ring, showed good AChE inhibition (IC_{50} = 0.118 μM) that was a little weaker than **1p** (IC_{50} = 0.036 μM). Of these compounds with a substituted aryl methyl at the *N*-atom of piperidine (**2c-q**), fluorophenyl-substituted compounds exhibited better AChE inhibitory activity (**2c-e**) but were still slightly weaker than the unsubstituted compound **1p**, indicating that the bulk groups at the phenyl ring of phenylpiperidine adversely affected AChE inhibition. Pyridyl-substituted compounds (**2i-k**) exhibited nearly 2-7 times weaker AChE inhibitory activity than **1p**, with IC_{50} values of 0.093, 0.261, 0.161 μM, respectively. Neither the electron-withdrawing (**2c-n**, **2q**) nor electron-donating group (**2o**, **2p**) was beneficial for AChE inhibition.

Taken together, diastereoisomers **1p** and **1w** were the most potent AChE inhibitors, exhibiting far more potency than the hit compound tadalafil, than the approved drug Hup A, and comparable potency to the best-selling anti-AD drug donepezil.

Compounds (**1p-q, 1v-w, 2b-e, 2i-k, 2m-n,** and **2q**) with good AChE inhibition (IC_{50} < 1 μM) were further assessed for their butyrylcholinesterase (BuChE)

inhibitory activities. The results shown in Table 3 indicated that these compounds had weaker BuChE inhibition and good AChE selectivity, and the selectivity index values for AChE varied from 17 to 273. Among these tested compounds, compounds with a cyano substituent at the phenyl ring of the phenylpiperidine fragment were very weak BuChE inhibitors, with 13.28-39.45% inhibition at 40 μM. Compounds with a fluoro or pyridyl substituent possessed moderate BuChE inhibitors, with IC_{50} values of 9.787-40.847 μM. Interestingly, increasing the chain length between 1-benzylpiperidine and the tadalafil parent nucleus led to increased BuChE inhibitory activities (IC_{50} values of **1p** *vs* **1q**: 9.835 *vs* 1.309 μM). The most potent AChE inhibitors, **1p** and **1w**, exhibited weak BuChE inhibitory activity, which was 273 and 121 times weaker than the AChE inhibitory activity, respectively, indicating that **1p** and **1w** were excellent selective AChE inhibitors over BuChE.

Table 3. *In vitro* BuChE inhibitory activities and selectivity for AChE of compounds **1p-q, 1v-w, 2b-e, 2i-k, 2m-n,** and **2q**[a].

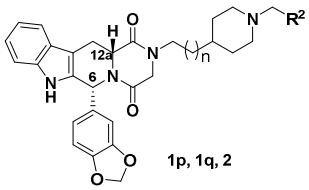

1p, 1q, 2

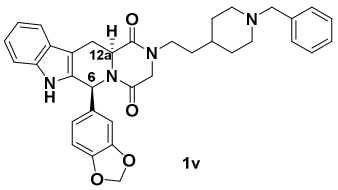

1v

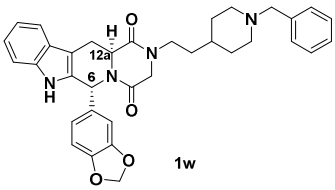

1w

Compd	R^2	n	IC_{50} ± SD (μM) for AChE	IC_{50} ± SD (μM) for BuChE[b] (Inhibition @ 40 μM)	SI[c]
1p	Ph	1	0.036 ± 0.008	9.835 ± 3.203	273
1q	Ph	2	0.075 ± 0.017	1.309 ± 0.012	17
1v	-	-	0.851 ± 0.129	16.200 ± 1.103	19
1w	-	-	0.032 ± 0.013	3.880 ± 0.275	121
2b	Cy	1	0.118 ± 0.029	3.977 ± 0.150	34
2c	2-fluorophenyl	1	0.067 ± 0.013	12.323 ± 0.554	184
2d	3-fluorophenyl	1	0.060 ± 0.014	13.725 ± 0.708	229
2e	4-fluorophenyl	1	0.089 ± 0.020	10.870 ± 1.454	122

2i	2-pyridyl	1	0.093 ± 0.008	9.787 ± 0.430	105
2j	3-pyridyl	1	0.261 ± 0.030	22.080 ± 1.784	85
2k	4-pyridyl	1	0.161 ± 0.016	40.847 ± 3.066	254
2m	3-cyanophenyl	1	0.800 ± 0.109	> 40 (27.12%)	> 50
2n	4-cyanophenyl	1	0.216 ± 0.045	> 40 (13.28%)	> 185
2q	3-nitrophenyl	1	0.833 ± 0.061	> 40 (39.45%)	> 48
Tadalafil	-	-	26.159 ± 1.300	> 40(3.86%)	> 1.53
Hup A	-	-	0.084 ± 0.017	36.400 ± 1.838	444
Donepezil	-	-	0.013 ± 0.150	7.704 ± 0.552	593

[a]BuChE from rat serum. [b]Results are expressed as the mean of at least three experiments. [c]Selectivity index for AChE is defined as IC_{50}(BuChE)/IC_{50}(AChE).

Phosphodiesterase 5 (PDE5) Inhibitory Activity

To evaluate whether these tadalafil derivatives retained PDE5 inhibition, an IMAP-FP (immobilized metal ion affinity-based fluorescence polarization) assay[54, 55] was conducted using tadalafil as a reference. Compounds (**1p-q, 1v-w, 2b-e, 2i-k, 2m-n,** and **2q**) with good AChE inhibition (IC_{50} < 1 μM) were selected to determine the PDE5 inhibitory activity to identify good dual-target AChE/PDE5 inhibitors, and the results are shown in Table 4. These data showed that most of the tested compounds could retain PDE5 inhibition, with IC_{50} values of 0.032-23.20 μM. The chain length between 1-benzylpiperidine and the tadalafil parent nucleus was no obvious influence on PDE5A1 inhibition (IC_{50} values of **1p** *vs* **1q**: 0.153 *vs* 0.150 μM). Compound **2b** with a six-membered nonaromatic ring substituent at the *N*-atom of piperidine and showed weaker PDE5A1 inhibition than the six-membered aromatic ring substituent (IC_{50} values of **1p** *vs* **2b**: 0.153 *vs* 0.335 μM).

Table 4. *In vitro* PDE5A1 inhibitory activities of compounds **1p-q, 1v-w, 2b-e, 2i-k, 2m-n,** and **2q**[a]**.**

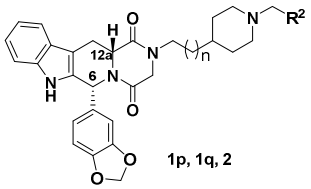

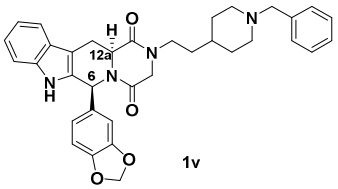

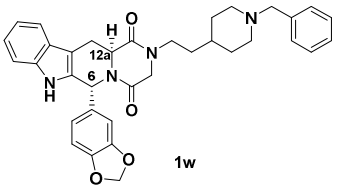

Compd	R^2	n	IC_{50} ± SD (μM)[a] for PDE5A1
1p	Ph	1	0.153 ± 0.005
1q	Ph	2	0.150 ± 0.420
1v	-	-	23.200 ± 7.040
1w	-	-	1.530 ± 0.004
2b	Cy	1	0.335 ± 0.261
2c	2-fluorophenyl	1	0.059 ± 0.086
2d	3-fluorophenyl	1	0.074 ± 0.021
2e	4-fluorophenyl	1	0.098 ± 0.021
2i	2-pyridyl	1	0.054 ± 0.010
2j	3-pyridyl	1	0.041 ± 0.005
2k	4-pyridyl	1	0.032 ± 0.013
2m	3-cyanophenyl	1	0.071 ± 0.006
2n	4-cyanophenyl	1	0.097 ± 0.008
2q	3-nitrophenyl	1	0.089 ± 0.016
Tadalafil	-	-	0.004 ± 0.0001
Donepezil	-	-	> 100

[a]Results are expressed as the mean of at least two experiments.

Compounds with a substituted aryl methyl at the *N*-atom of piperidine (**2c-e, 2i-k, 2m-n, 2q**) possessed better inhibitory activity than unsubstituted compound **1p**, indicating that the presence of bulk groups at the phenyl ring of phenylpiperidine was beneficial for PDE5A1 inhibition. Of these tested compounds, compounds (**2i-k**) with pyridyl substituents exhibited the best PDE5A1 inhibitory activity, with IC_{50} values of 0.054, 0.041, 0.032 μM, respectively. The most potent AChE inhibitors, **1p** and **1w**, exhibited good or moderate PDE5A1 inhibitory activity, with IC_{50} values of 0.153 μM

and 1.530 μM, respectively, indicating that **1p** and **1w** were good dual-target AChE/PDE5 inhibitors.

Noticeably, in the diastereoisomers **1p** (6*R*,12a*R*) and **1w** (6*R*,12a*S*), **1p** (6*R*,12a*R*) exhibited 10 times more potent PDE5A1 inhibitory activity (**1p**, IC_{50} = 0.153 μM; **1w**, IC_{50} = 1.530 μM), while in the diastereoisomers **1v** (6*S*,12a*S*) and **1w** (6*R*,12a*S*), **1w** (6*R*,12a*S*) showed 15.2 times more potent PDE5A1 inhibitory activity (**1v**, IC_{50} = 23.2 μM; **1w**, IC_{50} = 1.530 μM), demonstrating both the stereo-configurations at position 6 and 12 of the tadalafil parent nucleus, especially at position 6, were vital for exerting the strong PDE5A1 inhibitory activity, and the favored configuration was 6*R*, 12*R*.

SAR Studies

Based on the AChE and PDE5A1 inhibitory activity data shown in Tables 1-2 and 4, the noticeable SARs for compounds **1a-w** and **2a-q** were revealed as follows: (1) the chain length between the tadalafil parent nucleus and 1-benzylpiperidine exerted a large influence on the AChE inhibitory activities, with the potencies increasing in the order of zero methylene < one methylene < three methylene < two methylene (**1n** < **1o** < **1q** < **1p**), but no influence on the PDE5A1 inhibitory activities (**1p** *vs* **1q**); (2) the substituent pattern of benzylpiperidine was pivotal for AChE inhibition, and reversing the *N* atom position of 1-benzylpiperidine-4-ethyl led to almost no AChE inhibition (**1p** *vs* **1t**); (3) the stereo-configuration at position 6 of the tadalafil parent nucleus was key for displaying the strong AChE inhibitory activity, and the favored configuration was 6*R* (**1p** *vs* **1u** *vs* **1v** *vs* **1w**); (4) both the stereo-configurations at position 6 and 12 of the tadalafil parent nucleus, especially at position 6, were vital for exerting the strong PDE5A1 inhibitory activity, and the favored configuration was 6*R*, 12*R* (**1p** *vs* **1v** *vs* **1w**); (5) replacing phenyl with an aliphatic substituent (methyl or cyclohexyl) led to decreased inhibitions against both AChE (**2a**, **2b** *vs* **1p**) and PDE5A1 (**2b** *vs* **1p**); (6) bulk groups at the phenyl ring of phenylpiperidine showed an adverse effect on the AChE inhibition (**1p** *vs* **2c-q**) as opposite to a favorable effect on the PDE5A1 inhibition (**1p** *vs* **2c-e, 2i-k, 2m-n, 2q**).

In brief, the SARs of the 40 compounds were explicit and provided important insights into the key structural requirements for effective AChE/PDE5 inhibition.

Phosphodiesterase Selectivity Studies

Furthermore, the inhibitory activities of **1p** and **1w** against other PDE isoforms were also evaluated using an IMAP-FP assay. As shown in Table 5, **1p** and **1w** possessed no inhibitory activities against PDE2A1, PDE3A, PDE4D3, PDE6C, PDE7A and PDE9A2, demonstrating that they were highly selective PDE5 inhibitors.

Table 5. *In vitro* PDE2A1, PDE3A, PDE4D3, PDE6C, PDE7A and PDE9A2 inhibitory activities of compounds **1p** and **1w.**

Compd	IC_{50} ± SD (μM)[a]					
	PDE2A1	PDE3A	PDE4D3	PDE6C	PDE7A	PDE9A2
1p	> 100	> 100	> 100	> 100	> 100	> 100
1w	> 100	> 100	> 100	> 100	> 100	> 100
Trequinsin	1.062 ± 0.079	0.170 ± 0.001[b]	0.199 ± 0.021	n.t.[c]	n.t.[c]	n.t.[c]
Dipyridamole	n.t.[c]	n.t.[c]	n.t.[c]	0.943 ± 0.056	58.8 ± 3.21	n.t.[b]
Zaprinast	n.t.[c]	n.t.[c]	n.t.[c]	n.t.[c]	n.t.[c]	7.512 ± 0.687

[a]Results are expressed as the mean of at least two experiments. [b]unit: nM. [c]n.t. indicates no test.

***In Vitro* Blood-Brain Barrier Permeation Assay**

Good permeability of the BBB is an essential element for the development of anti-AD drugs. Compounds (**1p, 1q, 1w, 2b-e, 2i, 2k**) with good dual-target AChE/PDE5 inhibitors (AChE inhibition: IC_{50} < 0.2 μM; PDE5A1 inhibition: IC_{50} < 2 μM) were selected to determine their potential druggability and BBB penetrability.

The optimized compound BBB penetrabilities were evaluated by a parallel artificial membrane permeation assay (PAMPA) as described by Di *et al*[56]. First, the permeability (P_e) values of 13 commercial drugs *in vitro* were determined and compared with the reported values to validate the assay. A plot of the experimental data versus bibliographic values showed a good linear correlation, P_e (exp.) = 0.9738P_e (bibl.) – 0.8157 (R^2 = 0.9651, Figure S1, *Supporting Information*).

According to this equation and the threshold established by Di *et al*. for BBB permeation, we could conclude that compounds with P_e values over 3.08×10^{-6} cm s^{-1} could cross the BBB (CNS +); compounds with P_e values from 1.13×10^{-6} cm s^{-1} to 3.08×10^{-6} cm s^{-1} had uncertain BBB permeation (CNS ±); compounds with P_e values less than 1.13×10^{-6} cm s^{-1} were identified as CNS −, with low BBB permeation (Table S3, *Supporting Information*).

The P_e values of the tested compounds from the PAMPA-BBB assay and their prediction of BBB penetration are presented in Table 6. All the tested compounds exhibited good BBB permeation (CNS +), except compounds (**2i, 2k**) with pyridyl substituents, which showed uncertain BBB permeation. The P_e value of the hit compound, tadalafil, was 2.16, which indicated that tadalafil possessed poor BBB permeation. Compounds **1p**, **1q**, **1w** and **2b-e**, which possess a substituted or unsubstituted group on the phenyl ring of phenylpiperidine, have good BBB permeation (CNS +), indicating that it is successful for improving BBB permeation by introducing phenylpiperidine into tadalafil. Among them, compounds **1p** and **1w** exhibited better BBB permeability than **1q** and **2b-e**. Therefore, compounds **1p** and **1w**, the most potent AChE inhibitors with good PDE5 inhibitory activity and good druggability, were selected as the optimal dual-target AChE/PDE5 inhibitors for further study.

Table 6. Permeability results (P_e 10^{-6} cm s^{-1}) from the PAMPA-BBB assay for selected compounds **1p, 1q, 1w, 2b-e, 2i,** and **2k** and their prediction of BBB penetration.

Compd	P_e (10^{-6} cm s^{-1})[a]	Prediction[b]
1p	7.67 ± 1.21	CNS +
1q	6.98 ± 0.95	CNS +
1w	9.25 ± 0.93	CNS +
2b	7.92 ± 0.76	CNS +
2c	5.10 ± 0.05	CNS +
2d	5.39 ± 0.44	CNS +

2e	5.69 ± 0.41	CNS +
2i	3.06 ± 0.67	CNS ±
2k	2.74 ± 0.60	CNS ±
Tadalafil	2.16 ± 0.48	CNS ±
Donepezil	8.78 ± 2.24	CNS +

[a]PBS/EtOH (70:30) was used as the solvent.Values are expressed as the mean ± SD of at least three independent experiments. [b] CNS + : Compounds with $P_e > 3.08 \times 10^{-6}$ cm s^{-1} could cross the BBB by passive diffusion; CNS−: Compounds with $P_e < 1.13 \times 10^{-6}$ cm s^{-1} could not cross the BBB; CNS±: Compounds with 1.13×10^{-6} cm $s^{-1} < P_e < 3.08 \times 10^{-6}$ cm s^{-1} show uncertain BBB permeation.

Passageway Water Maze Test

To evaluate the *in vivo* effect of compounds **1p** and **1w** on cognitive improvement, the passageway water maze experiment was performed on a scopolamine (Scop)-induced cognitive deficit mouse model, a classical AD model to evaluate anticholinergic drug candidates,[57] with donepezil (Don) as a positive control (Ctrl).

As shown in Figure 3, the Scop group (model group) exhibited a longer escape latency and more frequent errors than the Ctrl group (negative group, $^{###}p < 0.001$). The groups treated with 10 mg/kg **1w·Cit** (citrate of **1w**) demonstrated a shorter escape latency and less frequent errors than the Scop group ($^{*}p < 0.05$), confirming that **1w·Cit** could relieve the Scop-induced learning and memory deficits at a dosage of 10 mg/kg, which was comparable to donepezil (no significant difference, $p > 0.05$). The groups treated with 10 mg/kg **1p·Cit** (citrate of **1p**) also demonstrated a shorter escape latency and less frequent errors than the Scop group, but this difference was not significant. Therefore, compound **1w·Cit** demonstrated the most potential as an AChE/PDE5 dual-target anti-AD lead compound due to its comparable effectivity with donepezil in the cognitive ability improvement of AD mouse model.

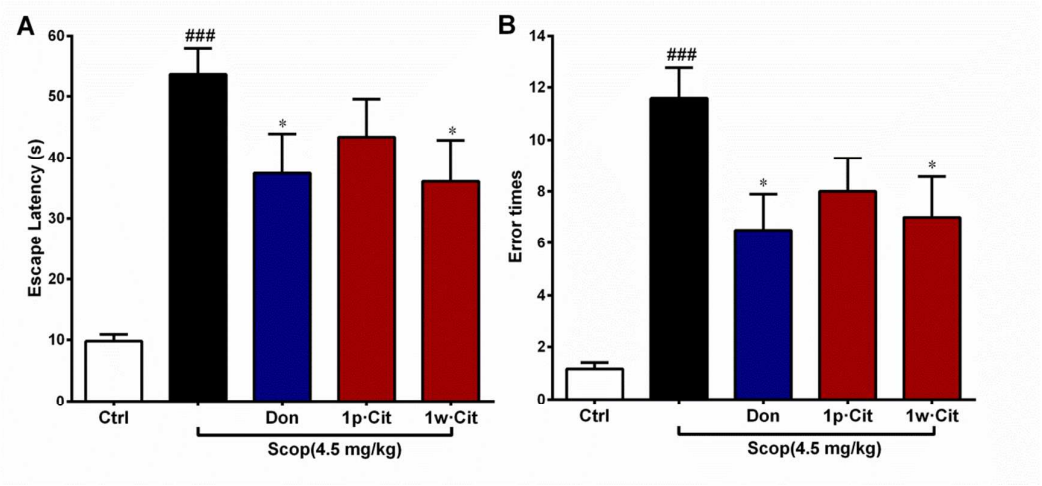

Figure 3. Effects of compounds **1p·Cit** and **1w·Cit** (10 mg/kg) on scopolamine-induced cognitive deficits in mice. Donepezil (10 mg/kg) as a reference. (A) The escape latency of mice in the passageway water maze. (B) The number of errors of mice in the passageway water maze. Data are shown as the mean ± SEM, $^{###}p < 0.001$ vs control group, $^{*}p < 0.05$ vs Scop group; N = 12. Ctrl group: solvent + saline; Scop group: solvent + scopolamine.

Western Blot Analysis

The inhibition of PDE5 led to an increase in cGMP levels, which promoted CREB phosphorylation (pCREB), a crucial factor in memory formation and synaptic plasticity.[24] Furthermore, PDE5 inhibition of **1p·Cit** and **1w·Cit** *in vivo* were confirmed by examining the level of pCREB-Ser133 (Figure 4). As expected, after administration of the PDE5 inhibitors **1p·Cit** and **1w·Cit** at 10 mg/kg, the levels of CREB phosphorylation were increased significantly, indicating that both optimal compounds could inhibit PDE5 *in vivo* and enhance CREB phosphorylation. Moreover, although PDE5 inhibition by **1p** *in vitro* was 10 times better than by **1w**, their levels of CREB phosphorylation were almost equivalent, 1.9 times and 1.8 times greater than the vehicle control (Ctrl), respectively. Taken together, the more effective compound (**1w·Cit**) for improving the cognitive dysfunction of Scop-induced cognitive deficit mice also exhibited an excellent effect on enhancing CREB

phosphorylation *in vivo*, which may ameliorate the cognitive impairment and restore synaptic function in AD.

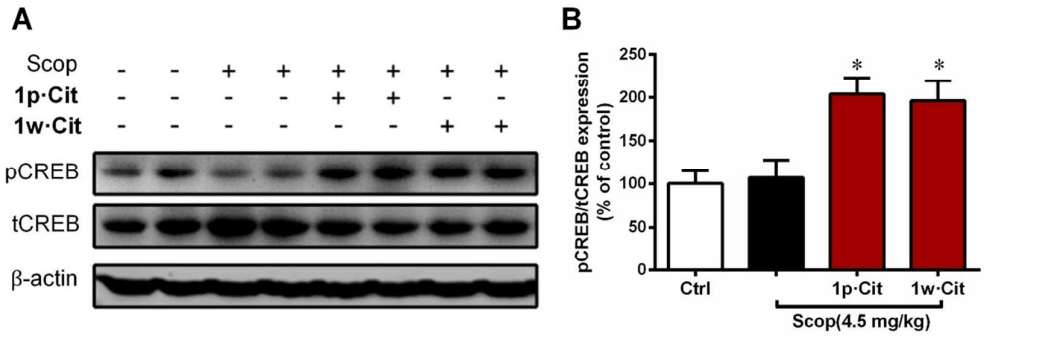

Figure 4. Effects of compounds **1p·Cit** and **1w·Cit** (10 mg/kg) on pCREB-Ser133 *in vivo*. (A) Representative bands in the western blot are shown. (B) The histogram shows the quantification of immunochemically reactive bands in the western blot. Data are the mean ± SEM, *p < 0.05 vs scopolamine group; N = 3. Ctrl group: solvent + saline; Scop group: solvent + scopolamine.

Molecular Docking Studies of 1w with AChE and PDE5

To explore the interaction mode of the optimal compound **1w** with AChE and PDE5, molecular docking simulation was performed using TriposSybyl 2.0 software based on the crystal structure of hAChE complexed with donepezil (PDB ID 4EY7[58]) and hPDE5A complexed tadalafil (PDB ID 2V60[59]), respectively.

As shown in Figure 5, compound **1w** could interact with both the catalytic active site (CAS) and peripheral anionic site (PAS) of hAChE. The benzylpiperidine fragment of compound **1w** bound to the bottom of the hAChE gorge (Figure 5A) and interacted with CAS via two cation-π stacking interactions and π-π stacking interactions. Specifically, the phenyl of the benzylpiperidine fragment interacted with Trp86 (4.0 Å) via face-to-face π-π stacking interactions, and the protonated *N* atom of the benzylpiperidine fragment interacted with Trp86 (4.9 Å) and Trp337 (5.6 Å) through cation-π stacking interactions. Importantly, in the mid-gorge site of hAChE, the carbonyl of the piperazinedione fragment participated in a hydrogen bond interaction with Phe295 (2.0 Å), while in the PAS of hAChE, the indole ring of **1w**

interacted with Trp286 (4.8 Å) via face-to-face π-π stacking interactions and the phenyl ring of benzo[*d*][1,3]dioxole fragment interacts with Trp341 (5.0 Å) via edge-to-face vertical π-π stacking interactions. In addition, the hexahydropyrazino[1',2':1,6]pyrido[3,4-*b*]indole-1,4-dione moiety bounds to the middle and external of the hAChE gorge, forming hydrophobic interactions with Trp286, Phe295 and Leu289 (Figure 5B).

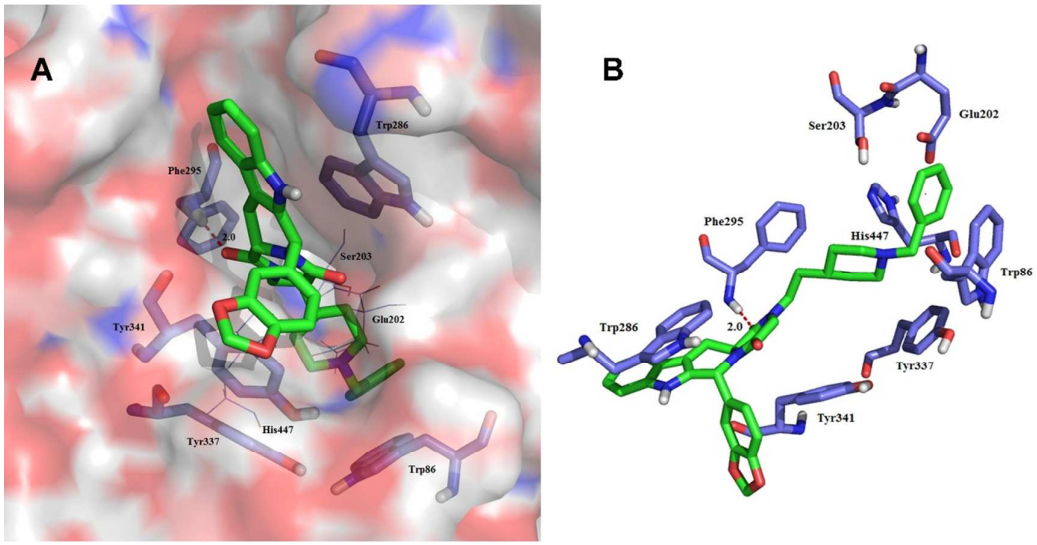

Figure 5. Predicted binding mode of compound **1w** with hAChE. (A) Surface representations of the binding mode of compound **1w** (carbon in green, oxygen in red, nitrogen in blue) within the active site pockets of hAChE. (B) 3D binding mode of compound **1w** within the active site pocket of hAChE. Hydrogen bonds are represented by dashed lines. The figures were generated using Pymol.

Additionally, the predicted binding mode of compound **1w** within the active site pockets of hPDE5A is presented in Figure 6. In general, compound **1w** contacts with Gln817, Phe820, Met816, Leu804 and Val782 of hPDE5A via a hydrogen bond and hydrophobic interactions. In detail, the benzo[*d*][1,3]dioxole fragment of **1w** occupies the hydrophobic pocket of hPDE5A, forming hydrophobic interactions with Met816, Leu804 and Val782. Furthermore, the indole fragment of **1w** interacts with the phenyl ring of Phe820 through face-to-face π-π stacking interactions (4.7 Å) and the NH of indole fragment interacts with Gln817 (2.1 Å) via hydrogen bond interactions.

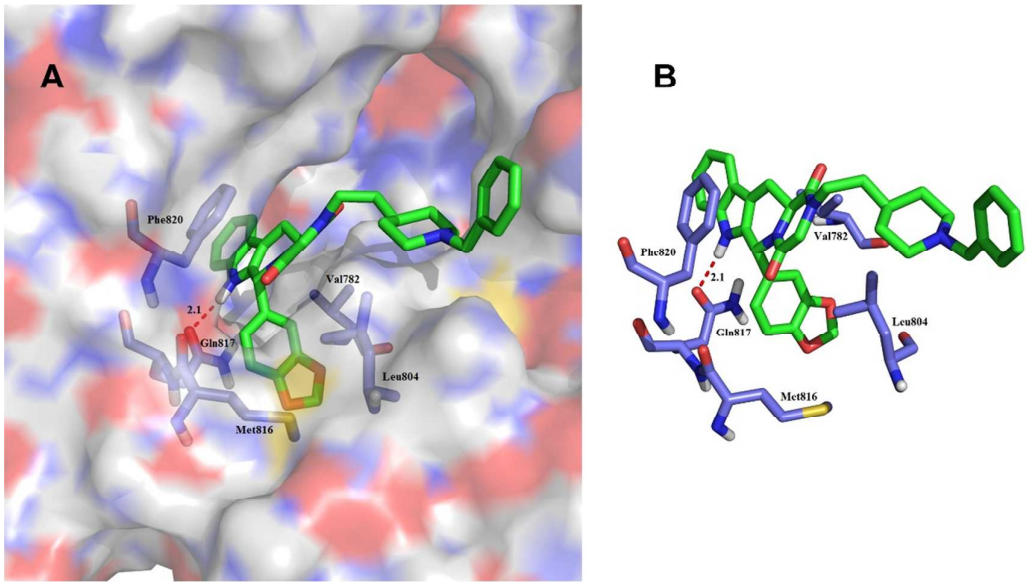

Figure 6. Predicted binding mode of compound **1w** with hPDE5A. (A) Surface representations of the binding mode of compound **1w** (carbon in green, oxygen in red, nitrogen in blue) within the active site pockets of hPDE5A. (B) 3D binding mode of compound **1w** within the active site pocket of hPDE5A. Hydrogen bonds are represented by dashed lines. The figures were generated using Pymol.

CONCLUSIONS

AChEs inhibitors remains the most successful means of improving the memory and cognitive function of AD patients, and PDE5 up-regulation in AD brains is an underlying magnetic AD therapeutic target. Therefore, AChE/PDE5 dual inhibitors may provide new perspectives and breakthroughs for the treatment of AD. Through screening of our old drug library, tadalafil, a selective PDE5 inhibitor, was found to have certain AChE inhibition.

To obtain good dual-target AChE/PDE5 inhibitors with improved AChE inhibitory activity and BBB penetrability, a series of tadalafil derivatives were rationally designed, synthesized and evaluated. The SAR studies revealed that the stereo-configuration at position 6 of the tadalafil parent nucleus was vital to display strong AChE inhibitory activity, and the favored configuration was 6*R*, while stereo-configuration at both position 6 and 12 of the tadalafil parent nucleus, especially position 6, was vital to exert strong PDE5A1 inhibitory activity, and the

favored configuration was 6*R*, 12*R*. Research has confirmed that **1p** and **1w** are excellent selective dual-target AChE/PDE5 inhibitors with improved BBB penetrability. Remarkably, **1w·Cit** demonstrated comparable effectivity with donepezil in cognitive ability improvement in the AD mouse model at a dosage of 10 mg/kg, and excellent effect on increasing the level of CREB phosphorylation *in vivo*, a crucial factor in ameliorating the cognitive impairment and restoring the synaptic function of AD. As CREB phosphorylation is a downstream effect of PDE5 inhibition, more studies will be needed to further determine the PDE inhibitory effect of **1w Cit** *in vivo*. Moreover, the molecular docking simulations of **1w** with hAChE and hPDE5A also confirmed the rationality of our design strategy.

In conclusion, a series of novel tadalafil derivatives with excellent selective dual-target AChE/PDE5 inhibitory activities and improved BBB penetrability were discovered through drug discovery strategies of repurposing and redeveloping existing drugs. The optimal compound **1w·Cit** could improve cognitive dysfunction in an AD mouse model and increase the level of CREB phosphorylation *in vivo*. Our research presents a potential selective dual-target AChE/PDE5 inhibitor as a good candidate drug for the treatment of AD, and they can also be regarded as an excellent molecule probe to explore the novel AD therapeutic approach *in vivo*.

EXPERIMENTAL SECTION

Chemistry. General Method. Reagents and solvents were purchased from Adamas-beta, Energy Chemical, J&K, TCI, and Target Molecule, which were used without further purification. Analytical thin-layer chromatography (TLC) was performed using HSGF 254 (150-200 μm thickness; Yantai Huiyou Co., China), and spots were visualized with UV light. Melting points were measured in capillary tubes on a SGW X-4 melting point apparatus without correction, and yields were not optimized. Nuclear magnetic resonance (NMR) spectroscopy was performed on a Bruker AMX-400 NMR. Chemical shifts were reported in parts per million (ppm, δ) downfield from tetramethylsilane. Proton coupling patterns were described as singlet (s), doublet (d), triplet (t), quartet (q), multiplet (m), and broad (br). High-resolution

mass spectra (HRMS) were obtained by electric ionization (EI) using a Waters GCT Premie and Waters LCT. HPLC data analysis of compounds **1a-t** and **2a-q** were performed on an Agilent 1100 with a quaternary pump and diode-array detector (DAD). The peak purity was verified by UV spectra. All analogs were confirmed to be ≥95% pure (Table S1, supporting information).

General procedure for the synthesis of target compounds 1a-1w. A solution of intermediate **4** (0.213 g, 0.5 mmol) and amine (1.2 equiv) in methanol (10 mL) with trimethylamine (1.5 equiv) was refluxed for 12-24 h and was monitored by TLC. After the reaction was complete, methanol was removed by evaporation. The residue was dissolved in dichloromethane. The organic layer was washed with saturated sodium bicarbonate solution and brine and dried over anhydrous sodium sulfate. Evaporation of the solvent gave a residue that was purified by chromatography with dichloromethane/methanol (40:1 – 10:1) as the eluent to afford the target compound.

(6*R*,12a*R*)-6-(benzo[*d*][1,3]dioxol-5-yl)-2-(2-morpholinoethyl)-2,3,6,7,12,12a-hexahydropyrazino[1',2':1,6]pyrido[3,4-*b*]indole-1,4-dione (1a). The intermediate and amine were **4a** and 2-morpholinoethan-1-amine, respectively. White solid, 62% yield, mp 248–249 °C. ^{1}H NMR (400 MHz, $CDCl_3$) δ 7.93 (s, 1H), 7.54 (d, *J* = 7.8 Hz, 1H), 7.33 (d, *J* = 8.1 Hz, 1H), 7.23 (t, *J* = 7.6 Hz, 1H), 7.17 (t, *J* = 7.4 Hz, 1H), 6.98 (s, 1H), 6.82 (s, 1H), 6.73 (s, 2H), 5.95 (s, 2H), 4.33 (t, *J* = 12.8 Hz, 2H), 4.06 (d, *J* = 17.5 Hz, 1H), 3.91 (s, 1H), 3.71 (s, 4H), 3.52 (dd, *J* = 15.3, 3.5 Hz, 1H), 3.24 (s, 1H), 2.99 (s, 1H), 2.60 (s, 6H). HRMS (EI) *m/z* calcd for $C_{27}H_{28}N_4O_5$ (M^+) 488.2060, found 488.2061.

(6*R*,12a*R*)-6-(benzo[*d*][1,3]dioxol-5-yl)-2-((*R*)-1-benzylpyrrolidin-3-yl)-2,3,6,7,12,12a-hexahydropyrazino[1',2':1,6]pyrido[3,4-*b*]indole-1,4-dione (1b).

The intermediate and amine were **4a** and (*R*)-1-benzylpyrrolidin-3-amine, respectively. White solid, 56% yield, mp 135–136 °C. ^{1}H NMR (400 MHz, $CDCl_3$) δ 8.13 (s, 1H), 7.62 – 7.09 (m, 4H), 7.05 – 6.61 (m, 4H), 5.91 (s, 2H), 5.16 (s, 1H), 4.27 (d, *J* = 20.2 Hz, 2H), 4.12 (d, *J* = 17.3 Hz, 1H), 3.73 – 3.37 (m, 3H), 3.12 – 2.42 (m, 3H), 2.26 (s, 2H), 1.82 (s, 2H). HRMS (EI) *m/z* calcd for $C_{32}H_{30}N_4O_4$ (M^+) 534.2267, found 534.2268.

(6*R*,12a*R*)-6-(benzo[*d*][1,3]dioxol-5-yl)-2-(2-(pyrrolidin-1-yl)ethyl)-2,3,6,7,12,12a-hexahydropyrazino[1',2':1,6]pyrido[3,4-*b*]indole-1,4-dione (1c). The intermediate and amine were **4a** and 2-(pyrrolidin-1-yl)ethan-1-amine. White solid, 53% yield, mp 278–280 °C. ^{1}H NMR (400 MHz, $CDCl_3$) δ 8.12 (s, 1H), 7.53 (d, *J* = 7.7 Hz, 1H), 7.31 (d, *J* = 8.0 Hz, 1H), 7.21 (t, *J* = 7.4 Hz, 1H), 7.15 (t, *J* = 7.4 Hz, 1H), 6.97 (s, 1H), 6.80 (s, 1H), 6.70 (s, 2H), 5.92 (d, *J* = 3.5 Hz, 2H), 4.39 – 4.24 (m, 2H), 4.10 (d, *J* = 17.7 Hz, 1H), 3.84 – 3.69 (m, 1H), 3.52 (dd, *J* = 15.4, 4.0 Hz, 1H), 3.42 – 3.27 (m, 1H), 3.03 – 2.90 (m, 1H), 2.73 (d, *J* = 4.6 Hz, 2H), 2.59 (s, 4H), 1.79 (s, 4H). HRMS (EI) *m/z* calcd for $C_{27}H_{28}N_4O_4$ (M^+) 472.2111, found 472.2164.

(6*S*,12a*R*)-6-(benzo[*d*][1,3]dioxol-5-yl)-2-(2-morpholinoethyl)-2,3,6,7,12,12a-hexa hydropyrazino[1',2':1,6]pyrido[3,4-*b*]indole-1,4-dione (1d). The intermediate and amine were **4b** and 2-morpholinoethan-1-amine, respectively. White solid, 58% yield, mp 147–150 °C. ^{1}H NMR (400 MHz, $CDCl_3$) δ 7.87 (s, 1H), 7.60 (d, *J* = 7.3 Hz, 1H), 7.28 (d, *J* = 7.6 Hz, 1H), 7.23 – 7.11 (m, 2H), 6.86 (d, *J* = 8.0 Hz, 1H), 6.74 (s, 1H), 6.69 (d, *J* = 8.0 Hz, 1H), 6.20 (s, 1H), 5.87 (d, *J* = 8.5 Hz, 2H), 4.45 – 4.14 (m, 2H), 4.05 – 3.89 (m, 1H), 3.88 – 3.48 (m, 6H), 3.41 (s, 1H), 3.22 (dd, *J* = 15.7, 11.7 Hz, 1H), 2.76 – 2.31 (m, 6H). HRMS (EI) *m/z* calcd for $C_{27}H_{28}N_4O_5$ (M^+) 488.2060, found 488.2059.

(6*S*,12a*R*)-6-(benzo[*d*][1,3]dioxol-5-yl)-2-((*R*)-1-benzylpyrrolidin-3-yl)-2,3,6,7,12, 12a-hexahydropyrazino[1',2':1,6]pyrido[3,4-*b*]indole-1,4-dione (1e). The intermediate and amine were **4b** and (*R*)-1-benzylpyrrolidin-3-amine, respectively. White solid, 60% yield, mp 138–140 °C. ^{1}H NMR (400 MHz, $CDCl_3$) δ 7.88 (s, 1H), 7.60 (d, *J* = 7.4 Hz, 1H), 7.35 – 7.27 (m, 1H), 7.22 – 7.12 (m, 2H), 6.84 (d, *J* = 7.6 Hz, 1H), 6.75 – 6.66 (m, 2H), 6.21 (s, 1H), 5.87 (d, *J* = 8.5 Hz, 2H), 5.21 (s, 1H), 4.45 (d, *J* = 17.2 Hz, 1H), 4.24 (dd, *J* = 11.4, 4.6 Hz, 1H), 3.97 (d, *J* = 17.7 Hz, 1H), 3.69 (dd, *J* = 15.9, 4.8 Hz, 2H), 3.49 (s, 1H), 3.22 (dd, *J* = 15.9, 11.5 Hz, 1H), 3.00 (s, 1H), 2.72 (s, 1H), 2.51 – 2.03 (m, 4H). HRMS (EI) *m/z* calcd for $C_{32}H_{30}N_4O_4$ (M^+) 534.2267, found 534.2269.

(6*S*,12a*R*)-6-(benzo[*d*][1,3]dioxol-5-yl)-2-(2-(pyrrolidin-1-yl)ethyl)-2,3,6,7,12,12a-hexahydropyrazino[1',2':1,6]pyrido[3,4-*b*]indole-1,4-dione (1f). The intermediate

and amine were **4b** and 2-(pyrrolidin-1-yl)ethan-1-amine, respectively. White solid, 52% yield, mp 140–142 °C. ^{1}H NMR (400 MHz, $CDCl_3$) δ 7.93 (s, 1H), 7.54 (d, *J* = 7.8 Hz, 1H), 7.33 (d, *J* = 8.1 Hz, 1H), 7.23 (t, *J* = 7.6 Hz, 1H), 7.17 (t, *J* = 7.4 Hz, 1H), 6.98 (s, 1H), 6.82 (s, 1H), 6.73 (s, 2H), 5.95 (s, 2H), 4.33 (t, *J* = 12.8 Hz, 2H), 4.06 (d, *J* = 17.5 Hz, 1H), 3.91 (s, 1H), 3.71 (s, 4H), 3.52 (dd, *J* = 15.3, 3.5 Hz, 1H), 3.24 (s, 1H), 2.99 (s, 1H), 2.60 (s, 6H). HRMS (EI) *m/z* calcd for $C_{27}H_{28}N_4O_4$ (M^+) 472.2111, found 472.2155.

(6*R*,12a*R*)-6-(benzo[*d*][1,3]dioxol-5-yl)-2-(1-benzylpyrrolidin-3-yl)-2,3,6,7,12,12a-hexahydropyrazino[1',2':1,6]pyrido[3,4-*b*]indole-1,4-dione (1g). The intermediate and amine were **4a** and 1-benzylpyrrolidin-3-amine, respectively. White solid, 59% yield, mp 129–131 °C. ^{1}H NMR (400 MHz, $CDCl_3$) δ 8.00 (s, 1H), 7.59 (d, *J* = 7.4 Hz, 1H), 7.29 (d, *J* = 7.6 Hz, 1H), 7.22 – 7.10 (m, 2H), 6.83 (d, *J* = 7.8 Hz, 1H), 6.71 (s, 1H), 6.68 (d, *J* = 7.8 Hz, 1H), 6.21 (s, 1H), 5.86 (d, *J* = 7.2 Hz, 2H), 5.16 (s, 1H), 4.37 (s, 1H), 4.25 (d, *J* = 6.4 Hz, 1H), 4.01 (d, *J* = 17.0 Hz, 1H), 3.68 (d, *J* = 15.9 Hz, 2H), 3.31 – 3.12 (m, 1H), 2.97 (d, *J* = 83.1 Hz, 2H), 2.32 (s, 2H), 1.93 – 1.66 (s, 3H). HRMS (EI) *m/z* calcd for $C_{32}H_{30}N_4O_4$ (M^+) 534.2267, found 534.2272.

(6*R*,12a*R*)-6-(benzo[*d*][1,3]dioxol-5-yl)-2-(2-(4-methylpiperazin-1-yl)ethyl)-2,3,6,7,12,12a-hexahydropyrazino[1',2':1,6]pyrido[3,4-*b*]indole-1,4-dione (1h). The intermediate and amine were **4a** and 2-(4-methylpiperazin-1-yl)ethan-1-amine, respectively. White solid, 56% yield, mp 189–190 °C. ^{1}H NMR (400 MHz, $CDCl_3$) δ 7.88 (s, 1H), 7.61 (d, *J* = 7.3 Hz, 1H), 7.30 (d, *J* = 7.6 Hz, 1H), 7.25 – 7.12 (m, 2H), 6.86 (d, *J* = 8.1 Hz, 1H), 6.72 (dd, *J* = 17.6, 4.7 Hz, 2H), 6.21 (s, 1H), 5.88 (d, *J* = 11.9 Hz, 2H), 4.34 (d, *J* = 6.3 Hz, 1H), 4.22 (d, *J* = 17.0 Hz, 1H), 3.94 (d, *J* = 17.1 Hz, 1H), 3.72 (dd, *J* = 16.1, 4.9 Hz, 1H), 3.67 (s, 2H), 3.24 (dd, *J* = 15.9, 11.8 Hz, 1H), 2.75 – 2.35 (m, 10H). HRMS (EI) *m/z* calcd for $C_{28}H_{31}N_5O_4$ (M^+) 501.2376, found 501.2375.

(6*R*,12a*R*)-6-(benzo[*d*][1,3]dioxol-5-yl)-2-(2-(piperidin-1-yl)ethyl)-2,3,6,7,12,12a-hexahydropyrazino[1',2':1,6]pyrido[3,4-*b*]indole-1,4-dione (1i). The intermediate and amine were **4a** and 2-(piperidin-1-yl)ethan-1-amine, respectively. White solid, 48% yield, mp 130–131 °C. ^{1}H NMR (400 MHz, $CDCl_3$) δ 7.87 (s, 1H), 7.60 (d, *J* = 6.8 Hz,

1H), 7.29 (d, *J* = 1.4 Hz, 1H), 7.16 (tt, *J* = 7.2, 5.7 Hz, 2H), 6.86 (dd, *J* = 8.0, 1.7 Hz, 1H), 6.74 (d, *J* = 1.7 Hz, 1H), 6.69 (d, *J* = 8.0 Hz, 1H), 6.19 (s, 1H), 5.87 (dd, *J* = 8.5, 1.3 Hz, 2H), 4.39 (s, 2H), 3.97 (d, *J* = 16.7 Hz, 1H), 3.74 (dd, *J* = 16.0, 4.7 Hz, 1H), 3.36 (s, 1H), 3.21 (dd, *J* = 15.8, 11.6 Hz, 1H), 2.53 (d, *J* = 59.9 Hz, 5H), 1.52 (d, *J* = 63.8 Hz, 8H). HRMS (EI) *m/z* calcd for $C_{25}H_{26}N_4O_4$ (M^+) 486.2267 found 486.2270.

(6*R*,12a*R*)-6-(benzo[*d*][1,3]dioxol-5-yl)-2-(2-(dimethylamino)ethyl)-2,3,6,7,12,12a-hexahydropyrazino[1',2':1,6]pyrido[3,4-*b*]indole-1,4-dione (1j). The intermediate and amine were **4a** and N^1,N^1-dimethylethane-1,2-diamine, respectively. White solid, 53% yield, mp 131–133 °C. ^{1}H NMR (400 MHz, $CDCl_3$) δ 7.87 (s, 1H), 7.59 (d, *J* = 7.1 Hz, 1H), 7.29 (s, 1H), 7.22 – 7.11 (m, 2H), 6.86 (dd, *J* = 8.0, 1.5 Hz, 1H), 6.74 (d, *J* = 1.5 Hz, 1H), 6.69 (d, *J* = 8.0 Hz, 1H), 6.18 (s, 1H), 5.87 (d, *J* = 8.3 Hz, 2H), 4.39 (d, *J* = 32.5 Hz, 2H), 3.97 (d, *J* = 17.3 Hz, 2H), 3.75 (dd, *J* = 15.9, 4.8 Hz, 1H), 3.34 – 3.12 (m, 2H), 2.59 (s, 2H), 2.36 (s, 6H). HRMS (EI) *m/z* calcd for $C_{25}H_{26}N_4O_4$ (M^+) 446.1954, found 446.1956.

(6*R*,12a*R*)-6-(benzo[*d*][1,3]dioxol-5-yl)-2-(2-(diethylamino)ethyl)-2,3,6,7,12,12a-hexahydropyrazino[1',2':1,6]pyrido[3,4-*b*]indole-1,4-dione (1k). The intermediate and amine were **4a** and N^1,N^1-diethylethane-1,2-diamine, respectively. White solid, 50% yield, mp 135–137 °C. ^{1}H NMR (400 MHz, $CDCl_3$) δ 8.05 (s, 1H), 7.66 – 7.54 (m, 1H), 7.28 (d, *J* = 1.6 Hz, 1H), 7.21 – 7.11 (m, 2H), 6.83 (dd, *J* = 8.0, 1.6 Hz, 1H), 6.73 (d, *J* = 1.5 Hz, 1H), 6.67 (d, *J* = 8.0 Hz, 1H), 6.17 (s, 1H), 5.85 (d, *J* = 7.3 Hz, 2H), 4.40 – 4.20 (m, 2H), 4.08 (d, *J* = 17.4 Hz, 1H), 3.74 (dd, *J* = 16.0, 4.6 Hz, 1H), 3.70 – 3.60 (m, 1H), 3.45 – 3.33 (m, 1H), 3.21 (dd, *J* = 15.7, 11.6 Hz, 1H), 2.67 (d, *J* = 5.8 Hz, 2H), 2.54 (d, *J* = 6.7 Hz, 4H), 0.99 (t, *J* = 7.1 Hz, 6H). HRMS (EI) *m/z* calcd for $C_{27}H_{30}N_4O_4$ (M^+) 474.2264 found 474.2269

(6*R*,12a*R*)-6-(benzo[*d*][1,3]dioxol-5-yl)-2-(2-(methyl(phenyl)amino)ethyl)-2,3,6,7,12,12a-hexahydropyrazino[1',2':1,6]pyrido[3,4-*b*]indole-1,4-dione (1l). The intermediate and amine were **4a** and N^1-methyl- N^1-phenylethane-1,2-diamine, respectively. White solid, 55% yield, mp 121–123 °C. ^{1}H NMR (400 MHz, $CDCl_3$) δ 8.04 (s, 1H), 7.60 (d, *J* = 6.9 Hz, 1H), 7.19 (ddd, *J* = 16.3, 15.3, 9.2 Hz, 5H), 6.88 – 6.58 (m, 6H), 6.09 (s, 1H), 5.84 (d, *J* = 8.5 Hz, 2H), 4.16 – 4.02 (m, 2H), 3.92 – 3.65

(m, 4H), 3.63 – 3.36 (m, 2H), 3.17 (dd, *J* = 15.7, 11.6 Hz, 1H), 2.94 (s, 3H). HRMS (EI) *m/z* calcd for $C_{30}H_{28}N_4O_4$ (M^+) 508.2111 found 508.2110.

(6*R*,12a*R*)-6-(benzo[*d*][1,3]dioxol-5-yl)-2-(2-(benzyl(methyl)amino)ethy)-2,3,6,7,12,12a-hexahydropyrazino[1',2':1,6]pyrido[3,4-*b*]indole-1,4-dione (1m). The intermediate and amine were **4a** and N^1-benzyl- N^1-methylethane-1,2-diamine, respectively. White solid, 53% yield, mp 84–86 °C. ^{1}H NMR (400 MHz, $CDCl_3$) δ 7.88 (s, 1H), 7.60 (d, *J* = 6.8 Hz, 1H), 7.29 (s, 1H), 7.22 – 7.11 (m, 2H), 6.86 (d, *J* = 8.0 Hz, 1H), 6.74 (s, 1H), 6.68 (d, *J* = 7.9 Hz, 1H), 6.18 (s, 1H), 5.85 (d, *J* = 4.8 Hz, 2H), 4.60 (s, 1H), 4.31 (s, 2H), 3.91 (d, *J* = 16.8 Hz, 2H), 3.73 (d, *J* = 15.8 Hz, 2H), 3.31 (d, *J* = 14.1 Hz, 1H), 3.25 – 3.12 (m, 1H), 2.68 (s, 2H), 2.36 (s, 3H). HRMS (EI) *m/z* calcd for $C_{31}H_{30}N_4O_4$ (M^+) 522.2267 found 522.2271.

(6*R*,12a*R*)-6-(benzo[*d*][1,3]dioxol-5-yl)-2-(1-benzylpiperidin-4-yl)-2,3,6,7,12,12a-hexahydropyrazino[1',2':1,6]pyrido[3,4-*b*]indole-1,4-dione (1n). The intermediate and amine were **4a** and 1-benzylpiperidin-4-amine, respectively. White solid, 65% yield, mp 151–153 °C. ^{1}H NMR (400 MHz, $CDCl_3$) δ 7.91 (s, 1H), 7.61 (d, *J* = 7.0 Hz, 1H), 7.29 (d, *J* = 7.2 Hz, 1H), 7.17 (dq, *J* = 7.2, 5.8 Hz, 2H), 6.84 (dd, *J* = 8.0, 1.7 Hz, 1H), 6.70 (d, *J* = 1.6 Hz, 1H), 6.68 (d, *J* = 8.0 Hz, 1H), 6.19 (s, 1H), 5.86 (dd, *J* = 8.6, 1.3 Hz, 2H), 4.54 (s, 1H), 4.28 (dd, *J* = 11.4, 4.6 Hz, 1H), 4.06 (d, *J* = 17.4 Hz, 1H), 3.89 (d, *J* = 17.1 Hz, 1H), 3.72 (dd, *J* = 16.1, 4.7 Hz, 2H), 3.20 (dd, *J* = 15.4, 11.6 Hz, 2H), 2.25 (s, 2H), 1.68 (d, *J* = 54.8 Hz, 6H). HRMS (EI) *m/z* calcd for $C_{33}H_{32}N_4O_4$ (M^+) 548.2424 found 548.2423.

(6*R*,12a*R*)-6-(benzo[*d*][1,3]dioxol-5-yl)-2-((1-benzylpiperidin-4-yl)methyl)-2,3,6,7,12,12a-hexahydropyrazino[1',2':1,6]pyrido[3,4-*b*]indole-1,4-dione (1o). The intermediate and amine were **4a** and (1-benzylpiperidin-4-yl)methanamine, respectively. White solid, 58% yield, mp 114–116 °C. ^{1}H NMR (400 MHz, $CDCl_3$) δ 8.02 (s, 1H), 7.59 (d, *J* = 7.2 Hz, 1H), 7.36 – 7.22 (m, 7H), 7.22 – 7.10 (m, 2H), 6.81 (d, *J* = 8.0 Hz, 1H), 6.71 (s, 1H), 6.66 (d, *J* = 7.9 Hz, 1H), 6.19 (s, 1H), 5.83 (d, *J* = 6.6 Hz, 2H), 4.29 (d, *J* = 10.8 Hz, 1H), 4.10 (d, *J* = 17.8 Hz, 1H), 3.90 (d, *J* = 17.3 Hz, 1H), 3.71 (d, *J* = 13.7 Hz, 1H), 3.43 (dd, *J* = 13.7, 7.5 Hz, 1H), 3.33 – 3.12 (m, 2H), 2.88 (d, *J* = 8.3 Hz, 2H), 1.96 (t, *J* = 10.8 Hz, 2H), 1.84 – 1.64 (m, 5H), 1.44 – 1.32

(m, 2H). HRMS (EI) *m/z* calcd for $C_{34}H_{34}N_4O_4$ (M^+) 562.2580 found 562.2582.

(6*R*,12a*R*)-6-(benzo[*d*][1,3]dioxol-5-yl)-2-(2-(1-benzylpiperidin-4-yl)ethyl)-2,3,6,7,12,12a-hexahydropyrazino[1',2':1,6]pyrido[3,4-*b*]indole-1,4-dione (1p). The intermediate and amine were **4a** and 2-(1-benzylpiperidin-4-yl)ethan-1-amine, respectively. White solid, 67% yield, mp 104-106 °C; ^{1}H NMR (400 MHz, $CDCl_3$) δ 7.92 (s, 1H), 7.60 (d, *J* = 7.3 Hz, 1H), 7.40 – 7.27 (m, 6H), 7.23 – 7.11 (m, 2H), 6.84 (dd, *J* = 8.0, 1.4 Hz, 1H), 6.72 (d, *J* = 1.3 Hz, 1H), 6.68 (d, *J* = 8.0 Hz, 1H), 6.17 (s, 1H), 5.86 (d, *J* = 7.9 Hz, 2H), 4.29 (dd, *J* = 11.5, 4.5 Hz, 1H), 4.07 (d, *J* = 17.3 Hz, 1H), 3.90 (d, *J* = 17.4 Hz, 1H), 3.74 (dd, *J* = 16.0, 4.6 Hz, 1H), 3.67 – 3.47 (m, 3H), 3.45 – 3.32 (m, 1H), 3.21 (dd, *J* = 15.8, 11.5 Hz, 1H), 2.93 (s, 2H), 2.03 (d, *J* = 17.6 Hz, 2H), 1.71 (s, 2H), 1.52 (dd, *J* = 14.1, 7.1 Hz, 2H), 1.34 (d, *J* = 40.9 Hz, 3H). ^{13}C NMR (126 MHz, $CDCl_3$) δ 167.13, 166.22, 147.72, 146.98, 137.94, 136.44, 135.27, 132.82, 129.25, 128.12, 126.98, 126.06, 122.29, 120.41, 119.91, 118.47, 111.22, 108.14, 107.38, 106.19, 101.06, 63.26, 56.26, 56.13, 53.50, 50.00, 44.03, 33.40, 33.26, 31.92, 23.40. HRMS (EI) *m/z* calcd for $C_{35}H_{38}N_4O_4$ (M^+) 576.3737, found 576.2738.

(6*R*,12a*R*)-6-(benzo[*d*][1,3]dioxol-5-yl)-2-(3-(1-benzylpiperidin-4-yl)propyl)-2,3,6,7,12,12a-hexahydropyrazino[1',2':1,6]pyrido[3,4-*b*]indole-1,4-dione (1q). The intermediate and amine were **4a** and 3-(1-benzylpiperidin-4-yl)propan-1-amine, respectively. White solid, 26% yield, mp 77-80 °C; ^{1}H NMR (400 MHz, $CDCl_3$) δ 7.91 (s, 1H), 7.60 (d, *J* = 7.4 Hz, 1H), 7.40 – 7.27 (m, 6H), 7.22 – 7.11 (m, 2H), 6.85 (d, *J* = 8.1 Hz, 1H), 6.73 (s, 1H), 6.69 (d, *J* = 8.0 Hz, 1H), 6.18 (s, 1H), 5.87 (d, *J* = 7.7 Hz, 2H), 4.30 (dd, *J* = 11.6, 4.0 Hz, 1H), 4.08 (d, *J* = 17.4 Hz, 1H), 3.91 (d, *J* = 17.6 Hz, 1H), 3.81 (dd, *J* = 40.5, 5.1 Hz, 1H), 3.74 – 3.66 (m, 3H), 3.56 (d, *J* = 13.3 Hz, 2H), 3.37 – 3.16 (m, 2H), 2.92 (d, *J* = 10.0 Hz, 2H), 2.00 (s, 2H), 1.59 (d, *J* = 7.6 Hz, 4H), 1.33 (s, 3H). HRMS (EI) *m/z* calcd for $C_{35}H_{38}N_4O_4$ (M^+) 590.2893, found 590.2894.

(6*R*,12a*R*)-2-(2-(1*H*-benzo[*d*]imidazol-1-yl)ethyl)-6-(benzo[*d*][1,3]dioxol-5-yl)-2,3,6,7,12,12a-hexahydropyrazino[1',2':1,6]pyrido[3,4-*b*]indole-1,4-dione (1r). The intermediate and amine were **4a** and 2-(1*H*-benzo[*d*]imidazol-1-yl)ethan-1-amine, respectively. White solid, 41% yield, mp 154–155 °C. ^{1}H NMR (400 MHz, $CDCl_3$) δ

8.35 (d, *J* = 48.2 Hz, 1H), 7.96 (d, *J* = 6.3 Hz, 1H), 7.82 – 7.75 (m, 1H), 7.61 – 7.41 (m, 2H), 7.36 – 7.10 (m, 5H), 6.83 (s, 1H), 6.78 – 6.60 (m, 3H), 6.08 (s, 1H), 5.93 (s, 1H), 5.83 (d, *J* = 9.9 Hz, 1H), 4.64 – 4.50 (m, 1H), 4.43 (dt, *J* = 20.0, 5.7 Hz, 1H), 4.36 – 4.23 (m, 1H), 4.07 – 3.88 (m, 1H), 3.74 – 3.54 (m, 3H), 3.42 (dd, *J* = 9.0, 4.6 Hz, 1H), 3.15 (dd, *J* = 15.9, 11.7 Hz, 1H), 2.85 – 2.72 (m, 1H). HRMS (EI) *m/z* calcd for $C_{30}H_{25}N_5O_4$ (M^+) 519.1907 found 519.1908.

(6R,12a*R*)-2-(2-(1*H*-imidazol-1-yl)ethyl)-6-(benzo[*d*][1,3]dioxol-5-yl)-2,3,6,7,12,12a-hexahydropyrazino[1',2':1,6]pyrido[3,4-*b*]indole-1,4-dione (1s). The intermediate and amine were **4a** and 2-(1*H*-imidazol-1-yl)ethan-1-amine, respectively. White solid, 35% yield, mp 153–155 °C. ^{1}H NMR (400 MHz, $CDCl_3$) δ 7.73 (s, 1H), 7.51 (d, *J* = 7.6 Hz, 1H), 7.27 (d, *J* = 7.9 Hz, 1H), 7.13 – 6.93 (m, 4H), 6.84 – 6.76 (m, 2H), 6.76 – 6.68 (m, 1H), 6.20 (s, 1H), 5.87 (d, *J* = 5.2 Hz, 2H), 4.38 (dd, *J* = 11.5, 4.1 Hz, 1H), 4.30 (t, *J* = 5.4 Hz, 2H), 4.05 (d, *J* = 17.1 Hz, 1H), 3.97 – 3.87 (m, 1H), 3.82 – 3.68 (m, 2H), 3.58 (dd, *J* = 15.9, 4.7 Hz, 1H), 3.07 (dd, *J* = 15.6, 11.7 Hz, 1H). HRMS (EI) *m/z* calcd for $C_{26}H_{23}N_5O_4$ (M^+) 469.1750 found 469.1753.

(6*R*,12a*R*)-6-(benzo[*d*][1,3]dioxol-5-yl)-2-(2-(4-benzylpiperidin-1-yl)ethyl)-2,3,6,7,12,12a-hexahydropyrazino[1',2':1,6]pyrido[3,4-*b*]indole-1,4-dione (1t). The intermediate and amine were **4a** and 2-(4-benzylpiperidin-1-yl)ethan-1-amine, respectively. White solid, 56% yield, mp 113–114 °C. ^{1}H NMR (400 MHz, $CDCl_3$) δ 7.88 (s, 1H), 7.60 (d, *J* = 7.1 Hz, 1H), 7.33 – 7.23 (m, 6H), 7.17 (dd, *J* = 10.8, 6.8 Hz, 3H), 7.12 (d, *J* = 7.5 Hz, 2H), 6.86 (d, *J* = 8.0 Hz, 1H), 6.74 (s, 1H), 6.69 (d, *J* = 8.0 Hz, 1H), 6.19 (s, 1H), 5.86 (d, *J* = 6.6 Hz, 2H), 4.33 (s, 2H), 4.00 (d, *J* = 17.0 Hz, 1H), 3.74 (dd, *J* = 16.0, 4.8 Hz, 2H), 3.36 (s, 1H), 3.21 (dd, *J* = 15.7, 11.7 Hz, 1H), 2.88 (s, 2H), 2.52 (t, *J* = 12.1 Hz, 4H), 1.94 (s, 2H), 1.76 – 1.45 (s, 5H). HRMS (EI) *m/z* calcd for $C_{35}H_{36}N_4O_4$ (M^+) 576.2737, found 576.2734.

(6*S*,12a*R*)-6-(benzo[*d*][1,3]dioxol-5-yl)-2-(2-(1-benzylpiperidin-4-yl)ethyl)-2,3,6,7,12,12a-hexahydropyrazino[1',2':1,6]pyrido[3,4-*b*]indole-1,4-dione (1u). The intermediate and amine were **4b** and 2-(1-benzylpiperidin-4-yl)ethan-1-amine, respectively. White solid, 57% yield, mp 127-129 °C; ^{1}H NMR (400 MHz, $CDCl_3$) δ 7.97 (s, 1H), 7.53 (d, *J* = 7.8 Hz, 1H), 7.38 – 7.27 (m, 6H), 7.25 – 7.12 (m, 2H), 6.96

(s, 1H), 6.81 (s, 1H), 6.71 (d, *J* = 0.8 Hz, 2H), 5.93 (d, *J* = 1.8 Hz, 2H), 4.33 (dd, *J* = 11.8, 4.2 Hz, 1H), 4.15 – 4.06 (m, 1H), 3.96 (d, *J* = 17.7 Hz, 1H), 3.61 – 3.48 (m, 4H), 3.35 – 3.25 (m, 1H), 2.97 – 2.85 (m, 3H), 1.98 (s, 2H), 1.70 (s, 2H), 1.52 (dd, *J* = 14.0, 7.4 Hz, 2H), 1.30 (dd, *J* = 15.0, 7.6 Hz, 3H). HRMS (EI) *m/z* calcd for $C_{35}H_{36}N_4O_4$ (M^+) 576.2737, found 576.2738.

(6*S*,12a*S*)-6-(benzo[*d*][1,3]dioxol-5-yl)-2-(2-(1-benzylpiperidin-4-yl)ethyl)-2,3,6,7, 12,12a-hexahydropyrazino[1',2':1,6]pyrido[3,4-*b*]indole-1,4-dione (1v). The intermediate and amine were **4c** and 2-(1-benzylpiperidin-4-yl)ethan-1-amine, respectively. White solid, 64% yield, mp 119-120 °C; ^{1}H NMR (400 MHz, $CDCl_3$) δ 7.89 (s, 1H), 7.53 (d, *J* = 7.8 Hz, 1H), 7.42 – 7.27 (m, 6H), 7.23 (t, *J* = 7.5 Hz, 1H), 7.17 (t, *J* = 7.3 Hz, 1H), 6.97 (s, 1H), 6.82 (s, 1H), 6.72 (s, 2H), 5.94 (s, 2H), 4.33 (dd, *J* = 11.9, 4.1 Hz, 1H), 4.11 (d, *J* = 17.7 Hz, 1H), 3.96 (d, *J* = 17.7 Hz, 1H), 3.73 – 3.45 (m, 4H), 3.39 – 3.25 (m, 1H), 2.92 (dd, *J* = 15.2, 12.6 Hz, 3H), 2.05 (s, 2H), 1.72 (s, 2H), 1.53 (d, *J* = 6.7 Hz, 2H), 1.28 (d, *J* = 23.3 Hz, 3H). HRMS (EI) *m/z* calcd for $C_{35}H_{36}N_4O_4$ (M^+) 576.2737, found 576.2740.

(6*R*,12a*S*)-6-(benzo[*d*][1,3]dioxol-5-yl)-2-(2-(1-benzylpiperidin-4-yl)ethyl)-2,3,6,7, 12,12a-hexahydropyrazino[1',2':1,6]pyrido[3,4-*b*]indole-1,4-dione (1w). The intermediate and amine were **4d** and 2-(1-benzylpiperidin-4-yl)ethan-1-amine, respectively. White solid, 61% yield, mp 84-86 °C; ^{1}H NMR (400 MHz, $CDCl_3$) δ 7.89 (s, 1H), 7.60 (d, *J* = 7.3 Hz, 1H), 7.40 – 7.27 (m, 6H), 7.17 (dt, *J* = 13.9, 6.9 Hz, 2H), 6.85 (d, *J* = 7.9 Hz, 1H), 6.73 (s, 1H), 6.68 (d, *J* = 8.0 Hz, 1H), 6.17 (s, 1H), 5.87 (d, *J* = 8.6 Hz, 2H), 4.29 (dd, *J* = 11.4, 4.5 Hz, 1H), 4.07 (d, *J* = 17.4 Hz, 1H), 3.90 (d, *J* = 17.4 Hz, 1H), 3.71 (dd, *J* = 10.8, 5.1 Hz, 2H), 3.65 – 3.54 (m, 2H), 3.45 – 3.30 (m, 1H), 3.21 (dd, *J* = 16.1, 11.6 Hz, 1H), 2.91 (s, 2H), 1.98 (s, 2H), 1.70 (d, *J* = 3.3 Hz, 2H), 1.52 (dd, *J* = 13.7, 6.9 Hz, 2H), 1.31 (d, *J* = 19.7 Hz, 3H). ^{13}C NMR (101 MHz, $CDCl_3$) δ 165.10, 161.83, 148.14, 148.03, 138.07, 136.33, 132.03, 129.77, 129.33, 128.21, 127.06, 126.23, 122.74, 122.52, 120.06, 118.45, 111.18, 109.19, 109.02, 108.33, 101.37, 63.36, 53.59, 53.56, 52.52, 51.84, 49.34, 43.96, 33.53, 32.92, 32.09, 31.97, 27.62. HRMS (EI) *m/z* calcd for $C_{35}H_{36}N_4O_4$ (M^+) 576.2737, found 576.2740.

General procedure for the synthesis of target compounds 2a-q. To a solution of

compound **1p** (0.577 g, 1 mmol) in methanol (10 mL), 10% Pd/C (0.3 equiv, wetted with ca. 55% water) was added and the solution was stirred under H_2 at room temperature and atmospheric pressure overnight. After the reaction was complete, Pd/C was filtered out, and the filtrate was evaporated in vacuum to afford intermediate **5**. To a solution of intermediate **5** (0.097 g, 0.2 mmol) in acetonitrile (5 mL), K_2CO_3 (1.5 equiv) was added. After the solution was stirred for 10 min at room temperature, an electrophilic reagent (R^2CH_2Cl or R^2CH_2Br) was added. The mixture was filtered after stirring for 12-24 h at room temperature, and the filtrate was evaporated in vacuum to provide the crude product, which was purified by chromatography with dichloromethane/methanol (40:1 – 10:1) as the eluent to afford the target compound.

(6*R*,12a*R*)-6-(benzo[*d*][1,3]dioxol-5-yl)-2-(2-(1-ethylpiperidin-4-yl)ethyl)-2,3,6,7,12,12a-hexahydropyrazino[1',2':1,6]pyrido[3,4-*b*]indole-1,4-dione (2a). The electrophilic reagent was bromoethane. White solid, 58% yield, mp 142–144 °C. ^{1}H NMR (400 MHz, $CDCl_3$) δ 7.98 (s, 1H), 7.60 (d, *J* = 7.4 Hz, 1H), 7.29 (d, *J* = 7.9 Hz, 1H), 7.23 – 7.11 (m, 2H), 6.87 (d, *J* = 7.9 Hz, 1H), 6.78 – 6.65 (m, 2H), 6.20 (s, 1H), 5.87 (d, *J* = 9.9 Hz, 2H), 4.31 (dd, *J* = 11.3, 4.5 Hz, 1H), 4.09 (d, *J* = 17.4 Hz, 1H), 3.91 (d, *J* = 17.4 Hz, 1H), 3.73 (dd, *J* = 15.8, 4.7 Hz, 1H), 3.59 (dt, *J* = 14.2, 7.2 Hz, 1H), 3.49 – 3.38 (m, 1H), 3.21 (dd, *J* = 16.0, 11.6 Hz, 2H), 2.72 (s, 2H), 2.25 (s, 2H), 1.87 (d, *J* = 13.0 Hz, 2H), 1.68 (s, 2H), 1.57 (dd, *J* = 14.0, 7.0 Hz, 2H), 1.42 – 1.20 (m, 5H). HRMS (EI) *m/z* calcd for $C_{30}H_{34}N_4O_4$ (M^+) 514.2580, found 514.2582.

(6*R*,12a*R*)-6-(benzo[*d*][1,3]dioxol-5-yl)-2-(2-(1-(cyclohexylmethyl)piperidin-4-yl)ethyl)-2,3,6,7,12,12a-hexahydropyrazino[1',2':1,6]pyrido[3,4-*b*]indole-1,4-dione (2b). The electrophilic reagent was (bromomethyl)cyclohexane. White solid, 39% yield, mp 123-125 °C. ^{1}H NMR (400 MHz, $CDCl_3$) δ 7.94 (s, 1H), 7.60 (d, *J* = 7.3 Hz, 1H), 7.29 (d, *J* = 7.9 Hz, 1H), 7.23 – 7.12 (m, 2H), 6.86 (d, *J* = 8.0 Hz, 1H), 6.75 – 6.66 (m, 2H), 6.19 (s, 1H), 5.87 (d, *J* = 9.8 Hz, 2H), 4.30 (dd, *J* = 11.4, 4.5 Hz, 1H), 4.08 (d, *J* = 17.3 Hz, 1H), 3.90 (d, *J* = 17.4 Hz, 1H), 3.74 (dd, *J* = 16.0, 4.7 Hz, 1H), 3.66 – 3.51 (m, 1H), 3.48 – 3.35 (m, 1H), 3.28 – 2.97 (m, 3H), 2.36 (s, 2H), 2.08 – 1.30 (m, 20H). HRMS (EI) *m/z* calcd for $C_{35}H_{32}N_4O_4$ (M^+) 582.3206, found

582.3204.

(6*R*,12a*R*)-6-(benzo[*d*][1,3]dioxol-5-yl)-2-(2-(1-(2-fluorobenzyl)piperidin-4-yl)ethyl)-2,3,6,7,12,12a-hexahydropyrazino[1',2':1,6]pyrido[3,4-*b*]indole-1,4-dione (2c). The electrophilic reagent was 2-fluorobenzyl bromide. White solid, 67% yield, mp 107-110 °C. ^{1}H NMR (400 MHz, $CDCl_3$) δ 7.85 (s, 1H), 7.60 (d, *J* = 7.4 Hz, 1H), 7.39 (s, 1H), 7.29 (s, 1H), 7.21 – 7.07 (m, 3H), 7.03 (t, *J* = 9.2 Hz, 1H), 6.85 (d, *J* = 8.0 Hz, 1H), 6.72 (s, 1H), 6.68 (d, *J* = 8.0 Hz, 1H), 6.17 (s, 1H), 5.87 (d, *J* = 9.3 Hz, 2H), 4.30 (dd, *J* = 11.4, 4.5 Hz, 1H), 4.07 (d, *J* = 17.4 Hz, 1H), 3.90 (d, *J* = 17.4 Hz, 1H), 3.79 – 3.69 (m, 1H), 3.60 (dt, *J* = 14.8, 7.5 Hz, 3H), 3.44 – 3.33 (m, 1H), 3.21 (dd, *J* = 16.0, 11.6 Hz, 1H), 2.92 (s, 2H), 2.04 (s, 2H), 1.70 (s, 2H), 1.51 (dd, *J* = 13.9, 7.0 Hz, 2H), 1.31 (d, *J* = 19.8 Hz, 3H). HRMS (EI) *m/z* calcd for $C_{35}H_{35}FN_4O_4$ (M^+) 594.2642, found 594.2644.

(6*R*,12a*R*)-6-(benzo[*d*][1,3]dioxol-5-yl)-2-(2-(1-(3-fluorobenzyl)piperidin-4-yl)ethyl)-2,3,6,7,12,12a-hexahydropyrazino[1',2':1,6]pyrido[3,4-*b*]indole-1,4-dione (2d). The electrophilic reagent was 3-fluorobenzyl chloride. White solid, 59% yield, mp 103-105 °C. ^{1}H NMR (400 MHz, $CDCl_3$) δ 7.90 (s, 1H), 7.60 (d, *J* = 7.3 Hz, 1H), 7.29 (s, 1H), 7.17 (dt, *J* = 13.9, 7.0 Hz, 2H), 7.07 (t, *J* = 9.0 Hz, 2H), 6.94 (t, *J* = 8.1 Hz, 1H), 6.85 (d, *J* = 7.9 Hz, 1H), 6.72 (s, 1H), 6.68 (d, *J* = 8.0 Hz, 1H), 6.17 (s, 1H), 5.86 (d, *J* = 8.6 Hz, 2H), 4.30 (dd, *J* = 11.4, 4.4 Hz, 1H), 4.07 (d, *J* = 17.3 Hz, 1H), 3.91 (d, *J* = 17.4 Hz, 1H), 3.75 (dd, *J* = 16.0, 4.5 Hz, 1H), 3.67 – 3.54 (m, 1H), 3.49 (s, 2H), 3.44 – 3.34 (m, 1H), 3.21 (dd, *J* = 16.0, 11.7 Hz, 1H), 2.87 (s, 2H), 1.95 (s, 2H), 1.69 (s, 2H), 1.52 (dd, *J* = 13.7, 7.1 Hz, 2H), 1.31 (d, *J* = 20.1 Hz, 3H). HRMS (EI) *m/z* calcd for $C_{35}H_{35}FN_4O_4$ (M^+) 594.2642, found 594.2643.

(6*R*,12a*R*)-6-(benzo[*d*][1,3]dioxol-5-yl)-2-(2-(1-(4-fluorobenzyl)piperidin-4-yl)ethyl)-2,3,6,7,12,12a-hexahydropyrazino[1',2':1,6]pyrido[3,4-*b*]indole-1,4-dione (2e). The electrophilic reagent was 4-fluorobenzyl chloride. White solid, 64% yield, mp 95-97 °C. ^{1}H NMR (400 MHz, $CDCl_3$) δ 7.86 (s, 1H), 7.60 (d, *J* = 7.4 Hz, 1H), 7.28 (d, *J* = 7.9 Hz, 2H), 7.17 (dt, *J* = 14.1, 6.9 Hz, 2H), 7.00 (t, *J* = 8.5 Hz, 2H), 6.85 (d, *J* = 8.0 Hz, 1H), 6.73 (s, 1H), 6.69 (d, *J* = 8.0 Hz, 1H), 6.17 (s, 1H), 5.87 (d, *J* = 9.0 Hz, 2H), 4.30 (dd, *J* = 11.4, 4.5 Hz, 1H), 4.08 (d, *J* = 17.3 Hz, 1H), 3.91 (d, *J* = 17.4 Hz,

1H), 3.71 (dd, *J* = 10.8, 5.1 Hz, 2H), 3.65 – 3.54 (m, 1H), 3.49 (s, 1H), 3.44 – 3.33 (m, 1H), 3.21 (dd, *J* = 15.8, 11.5 Hz, 1H), 2.89 (s, 2H), 1.96 (s, 2H), 1.70 (d, *J* = 4.1 Hz, 2H), 1.52 (dd, *J* = 13.7, 7.0 Hz, 2H), 1.28 (s, 3H). HRMS (EI) *m/z* calcd for $C_{35}H_{35}FN_4O_4$ (M^+) 594.2642, found 594.2645.

(6*R*,12a*R*)-6-(benzo[*d*][1,3]dioxol-5-yl)-2-(2-(1-(3-chlorobenzyl)piperidin-4-yl)ethyl)-2,3,6,7,12,12a-hexahydropyrazino[1',2':1,6]pyrido[3,4-*b*]indole-1,4-dione (2f). The electrophilic reagent was 3-chlorobenzyl bromide. White solid, 68% yield, mp 162-164 °C. ^{1}H NMR (400 MHz, $CDCl_3$) δ 7.94 (s, 1H), 7.60 (s, 1H), 7.32 (s, 2H), 7.20 (d, *J* = 21.0 Hz, 4H), 6.83 (s, 1H), 6.70 (d, *J* = 15.1 Hz, 2H), 6.17 (s, 1H), 5.86 (d, *J* = 7.3 Hz, 2H), 4.29 (d, *J* = 11.1 Hz, 1H), 4.07 (d, *J* = 17.5 Hz, 1H), 3.90 (d, *J* = 17.3 Hz, 1H), 3.74 (d, *J* = 15.6 Hz, 1H), 3.58 (s, 1H), 3.43 (d, *J* = 25.8 Hz, 3H), 3.21 (t, *J* = 13.7 Hz, 1H), 2.85 (s, 2H), 1.95 (s, 2H), 1.69 (s, 2H), 1.51 (s, 2H), 1.26 (s, 3H). HRMS (EI) *m/z* calcd for $C_{35}H_{35}ClN_4O_4$ (M^+) 610.2347, found 610.2341.

(6*R*,12a*R*)-6-(benzo[*d*][1,3]dioxol-5-yl)-2-(2-(1-(3-bromobenzyl)piperidin-4-yl)ethyl)-2,3,6,7,12,12a-hexahydropyrazino[1',2':1,6]pyrido[3,4-*b*]indole-1,4-dione (2g). The electrophilic reagent was 3-bromobenzyl bromide. White solid, 55% yield, mp 122-124 °C. ^{1}H NMR (400 MHz, $CDCl_3$) ^{1}H NMR (400 MHz, $CDCl_3$) δ 7.89 (s, 1H), 7.62 – 7.56 (m, 1H), 7.48 (s, 1H), 7.39 (d, *J* = 7.6 Hz, 1H), 7.30 – 7.26 (m, 2H), 7.22 – 7.13 (m, 3H), 6.84 (dd, *J* = 8.0, 1.8 Hz, 1H), 6.72 (d, *J* = 1.7 Hz, 1H), 6.68 (d, *J* = 8.0 Hz, 1H), 6.17 (s, 1H), 5.86 (dd, *J* = 8.7, 1.4 Hz, 2H), 4.29 (dd, *J* = 11.5, 4.1 Hz, 1H), 4.07 (dd, *J* = 17.4, 1.2 Hz, 1H), 3.90 (d, *J* = 17.4 Hz, 1H), 3.74 (dd, *J* = 16.1, 4.7 Hz, 1H), 3.64 – 3.54 (m, 1H), 3.48 (s, 2H), 3.44 – 3.35 (m, 1H), 3.26 – 3.16 (m, 1H), 2.87 (s, 2H), 1.97 (s, 2H), 1.70 (s, 2H), 1.52 (dd, *J* = 13.9, 7.2 Hz, 2H), 1.31 (d, *J* = 19.8 Hz, 3H). HRMS (EI) *m/z* calcd for $C_{35}H_{35}BrN_4O_4$ (M^+) 654.1842, found 654.1840.

(6*R*,12a*R*)-6-(benzo[*d*][1,3]dioxol-5-yl)-2-(2-(1-(3-iodobenzyl)piperidin-4-yl)ethyl)-2,3,6,7,12,12a-hexahydropyrazino[1',2':1,6]pyrido[3,4-*b*]indole-1,4-dione (2h). The electrophilic reagent was 3-iodobenzyl bromide. White solid, 34% yield, mp 124-126 °C. ^{1}H NMR (400 MHz, $CDCl_3$) δ 7.87 (s, 1H), 7.68 (s, 1H), 7.60 (s, 2H), 7.33 (s, 1H), 7.17 (s, 2H), 7.05 (s, 1H), 6.84 (s, 1H), 6.71 (d, *J* = 11.6 Hz, 2H), 6.17 (s,

1H), 5.87 (d, *J* = 7.7 Hz, 2H), 4.30 (d, *J* = 10.9 Hz, 1H), 4.07 (d, *J* = 17.2 Hz, 1H), 3.91 (d, *J* = 17.4 Hz, 1H), 3.74 (d, *J* = 15.7 Hz, 1H), 3.58 (s, 1H), 3.44 (d, *J* = 19.3 Hz, 3H), 3.27 – 3.15 (m, 1H), 2.89 (s, 2H), 1.97 (s, 2H), 1.71 (s, 2H), 1.52 (s, 2H), 1.26 (s, 3H). HRMS (EI) *m/z* calcd for $C_{35}H_{35}IN_4O_4$ (M^+) 702.1703, found 702.1687.

(6*R*,12a*R*)-6-(benzo[*d*][1,3]dioxol-5-yl)-2-(2-(1-(pyridin-2-ylmethyl)piperidin-4-yl)ethyl)-2,3,6,7,12,12a-hexahydropyrazino[1',2':1,6]pyrido[3,4-*b*]indole-1,4-dione (2i). The electrophilic reagent was 2-(chloromethyl)pyridine hydrochloride. White solid, 43% yield, mp 105-106 °C. ^{1}H NMR (400 MHz, $CDCl_3$) δ 8.55 (d, *J* = 4.5 Hz, 1H), 7.99 (s, 1H), 7.71 – 7.55 (m, 2H), 7.45 (s, 1H), 7.29 (s, 1H), 7.16 (dd, *J* = 13.5, 6.7 Hz, 3H), 6.84 (d, *J* = 7.9 Hz, 1H), 6.77 – 6.63 (m, 2H), 6.18 (s, 1H), 5.89 (t, *J* = 16.3 Hz, 2H), 4.29 (dd, *J* = 11.5, 4.3 Hz, 1H), 4.07 (d, *J* = 17.5 Hz, 1H), 3.90 (d, *J* = 17.3 Hz, 1H), 3.80 – 3.53 (m, 4H), 3.47 – 3.32 (m, 1H), 3.21 (dd, *J* = 15.8, 11.7 Hz, 1H), 2.93 (s, 2H), 2.09 (s, 2H), 1.72 (d, *J* = 11.0 Hz, 2H), 1.56 – 1.32 (m, 5H). HRMS (EI) *m/z* calcd for $C_{34}H_{35}N_5O_4$ (M^+) 577.2689, found 577.2691.

(6*R*,12a*R*)-6-(benzo[*d*][1,3]dioxol-5-yl)-2-(2-(1-(pyridin-3-ylmethyl)piperidin-4-yl)ethyl)-2,3,6,7,12,12a-hexahydropyrazino[1',2':1,6]pyrido[3,4-*b*]indole-1,4-dione (2j). The electrophilic reagent was 3-(bromomethyl)pyridine hydrobromide. White solid, 37% yield, mp 138-140 °C. ^{1}H NMR (400 MHz, $CDCl_3$) δ 8.53 (s, 2H), 7.92 (s, 1H), 7.60 (d, *J* = 6.9 Hz, 1H), 7.28 (d, *J* = 7.2 Hz, 2H), 7.17 (dq, *J* = 7.1, 5.7 Hz, 2H), 6.85 (dd, *J* = 8.0, 1.7 Hz, 1H), 6.72 (d, *J* = 1.7 Hz, 1H), 6.69 (d, *J* = 8.0 Hz, 1H), 6.18 (s, 1H), 5.87 (dd, *J* = 9.4, 1.3 Hz, 2H), 4.30 (dd, *J* = 11.4, 4.4 Hz, 1H), 4.08 (d, *J* = 16.1 Hz, 1H), 3.90 (d, *J* = 17.3 Hz, 1H), 3.81 – 3.67 (m, 2H), 3.65 – 3.50 (m, 2H), 3.47 – 3.36 (m, 1H), 3.21 (dd, *J* = 15.1, 11.4 Hz, 1H), 2.96 (s, 2H), 1.75 (s, 2H), 1.64 (s, 2H), 1.54 (dd, *J* = 13.9, 6.9 Hz, 2H), 1.31 (d, *J* = 19.6 Hz, 3H). HRMS (EI) *m/z* calcd for $C_{34}H_{35}N_5O_4$ (M^+) 577.2689, found 577.2690.

(6*R*,12a*R*)-6-(benzo[*d*][1,3]dioxol-5-yl)-2-(2-(1-(pyridin-4-ylmethyl)piperidin-4-yl)ethyl)-2,3,6,7,12,12a-hexahydropyrazino[1',2':1,6]pyrido[3,4-*b*]indole-1,4-dione (2k). The electrophilic reagent was 4-(bromomethyl)pyridine hydrobromide. White solid, 41% yield, mp 141-143 °C. ^{1}H NMR (400 MHz, $CDCl_3$) δ 8.55 (s, 2H), 7.89 (s, 1H), 7.59 (s, 1H), 7.42 (s, 2H), 7.17 (s, 2H), 6.85 (s, 1H), 6.71 (d, *J* = 9.3 Hz, 2H),

6.18 (s, 1H), 5.87 (d, *J* = 9.1 Hz, 2H), 4.29 (s, 1H), 4.08 (d, *J* = 17.0 Hz, 1H), 3.91 (d, *J* = 16.6 Hz, 1H), 3.75 (d, *J* = 15.6 Hz, 1H), 3.50 (t, *J* = 28.8 Hz, 4H), 3.30 – 3.13 (m, 1H), 2.86 (s, 2H), 2.01 (s, 2H), 1.73 (s, 2H), 1.61 (s, 2H), 1.26 (s, 3H). HRMS (EI) *m/z* calcd for $C_{34}H_{35}N_5O_4$ (M^+) 577.2689, found 577.2684.

(6*R*,12a*R*)-6-(benzo[*d*][1,3]dioxol-5-yl)-2-(2-(1-(2-cyanobenzyl)piperidin-4-yl)ethyl)-2,3,6,7,12,12a-hexahydropyrazino[1',2':1,6]pyrido[3,4-*b*]indole-1,4-dione (2l). The electrophilic reagent was 2-cyanobenzyl bromide. White solid, 52% yield, mp 122-124 °C. ^{1}H NMR (400 MHz, $CDCl_3$) δ 7.95 (s, 1H), 7.69 – 7.51 (m, 4H), 7.34 (s, 1H), 7.16 (s, 2H), 6.83 (s, 1H), 6.72 (s, 1H), 6.68 (d, *J* = 7.6 Hz, 1H), 6.17 (s, 1H), 5.86 (d, *J* = 9.8 Hz, 2H), 4.29 (d, *J* = 11.3 Hz, 1H), 4.07 (d, *J* = 17.2 Hz, 1H), 3.90 (d, *J* = 17.5 Hz, 1H), 3.69 (dd, *J* = 43.2, 26.1 Hz, 4H), 3.40 (s, 1H), 3.21 (t, *J* = 13.5 Hz, 1H), 2.86 (s, 2H), 2.06 (d, *J* = 9.0 Hz, 2H), 1.69 (s, 2H), 1.52 (s, 2H), 1.28 (s, 3H). HRMS (EI) *m/z* calcd for $C_{36}H_{35}N_5O_4$ (M^+) 601.2689, found 601.2686.

(6*R*,12a*R*)-6-(benzo[*d*][1,3]dioxol-5-yl)-2-(2-(1-(3-cyanobenzyl)piperidin-4-yl)ethyl)-2,3,6,7,12,12a-hexahydropyrazino[1',2':1,6]pyrido[3,4-*b*]indole-1,4-dione (2m). The electrophilic reagent was 3-cyanobenzyl bromide. White solid, 48% yield, mp 124-127 °C. ^{1}H NMR (400 MHz, $CDCl_3$) δ 7.81 (s, 1H), 7.60 (dd, *J* = 22.9, 15.5 Hz, 3H), 7.42 (s, 1H), 7.28 (d, *J* = 7.8 Hz, 1H), 7.24 – 7.11 (m, 2H), 6.86 (d, *J* = 8.1 Hz, 1H), 6.73 (s, 1H), 6.69 (d, *J* = 8.0 Hz, 1H), 6.18 (s, 1H), 5.88 (d, *J* = 8.7 Hz, 2H), 4.30 (dd, *J* = 11.4, 4.5 Hz, 1H), 4.08 (d, *J* = 17.4 Hz, 1H), 3.91 (d, *J* = 17.3 Hz, 1H), 3.75 (dd, *J* = 16.1, 4.6 Hz, 1H), 3.66 – 3.34 (m, 4H), 3.22 (dd, *J* = 15.7, 11.9 Hz, 1H), 2.82 (s, 2H), 1.96 (s, 2H), 1.71 (s, 2H), 1.54 (s, 2H), 1.39 – 1.26 (m, 3H). HRMS (EI) *m/z* calcd for $C_{36}H_{35}N_5O_4$ (M^+) 601.2689, found 601.2679.

(6*R*,12a*R*)-6-(benzo[*d*][1,3]dioxol-5-yl)-2-(2-(1-(4-cyanobenzyl)piperidin-4-yl)ethyl)-2,3,6,7,12,12a-hexahydropyrazino[1',2':1,6]pyrido[3,4-*b*]indole-1,4-dione (2n). The electrophilic reagent was 4-cyanobenzyl chloride. White solid, 54% yield, mp 128-130 °C. ^{1}H NMR (400 MHz, $CDCl_3$) δ 7.86 (s, 1H), 7.60 (d, *J* = 6.2 Hz, 3H), 7.45 (s, 1H), 7.28 (d, *J* = 7.8 Hz, 1H), 7.23 – 7.12 (m, 2H), 6.85 (d, *J* = 8.0 Hz, 1H), 6.72 (s, 1H), 6.69 (d, *J* = 8.0 Hz, 1H), 6.17 (s, 1H), 5.87 (d, *J* = 8.8 Hz, 2H), 4.30 (dd, *J* = 11.5, 4.4 Hz, 1H), 4.08 (d, *J* = 17.4 Hz, 1H), 3.91 (d, *J* = 17.4 Hz, 1H), 3.75 (dd, *J*

= 16.1, 4.6 Hz, 1H), 3.65 – 3.46 (m, 3H), 3.46 – 3.35 (m, 1H), 3.21 (dd, *J* = 15.8, 11.7 Hz, 1H), 2.82 (s, 2H), 1.97 (s, 2H), 1.70 (s, 2H), 1.53 (d, *J* = 5.1 Hz, 2H), 1.27 (s, 3H). HRMS (EI) *m/z* calcd for $C_{36}H_{35}N_5O_4$ (M^+) 601.2689, found 601.2692.

(6*R*,12a*R*)-6-(benzo[*d*][1,3]dioxol-5-yl)-2-(2-(1-(4-methylbenzyl)piperidin-4-yl)ethyl)-2,3,6,7,12,12a-hexahydropyrazino[1',2':1,6]pyrido[3,4-*b*]indole-1,4-dione (2o). The electrophilic reagent was 4-methylbenzyl bromide. White solid, 50% yield, mp 110-111 °C. ^{1}H NMR (400 MHz, $CDCl_3$) δ 7.84 (s, 1H), 7.61 (d, *J* = 7.0 Hz, 1H), 7.29 (s, 1H), 7.24 – 7.09 (m, 5H), 6.85 (dd, *J* = 8.1, 1.5 Hz, 1H), 6.71 (dd, *J* = 15.6, 4.7 Hz, 2H), 6.17 (s, 1H), 5.88 (dd, *J* = 9.1, 1.2 Hz, 2H), 4.30 (dd, *J* = 11.3, 4.3 Hz, 1H), 4.07 (d, *J* = 17.0 Hz, 1H), 3.91 (d, *J* = 17.4 Hz, 1H), 3.75 (dd, *J* = 16.1, 4.6 Hz, 1H), 3.66 – 3.55 (m, 1H), 3.49 (s, 2H), 3.44 – 3.33 (m, 1H), 3.21 (dd, *J* = 15.3, 11.6 Hz, 1H), 2.90 (s, 2H), 2.34 (s, 3H), 1.94 (s, 2H), 1.70 (s, 2H), 1.52 (dd, *J* = 13.8, 6.9 Hz, 2H), 1.45 – 1.27 (m, 3H). HRMS (EI) *m/z* calcd for $C_{36}H_{38}N_4O_4$ (M^+) 590.2893, found 590.2891.

(6*R*,12a*R*)-6-(benzo[*d*][1,3]dioxol-5-yl)-2-(2-(1-(4-methoxylbenzyl)piperidin-4-yl)ethyl)-2,3,6,7,12,12a-hexahydropyrazino[1',2':1,6]pyrido[3,4-*b*]indole-1,4-dione (2p). The electrophilic reagent was 4-methoxylbenzyl chloride. White solid, 60% yield, mp 175-177 °C. ^{1}H NMR (400 MHz, $CDCl_3$) δ 8.05 (s, 1H), 7.59 (d, *J* = 7.3 Hz, 1H), 7.27 (d, *J* = 9.8 Hz, 4H), 7.16 (dt, *J* = 13.9, 6.8 Hz, 2H), 6.85 (t, *J* = 7.7 Hz, 3H), 6.72 (s, 1H), 6.67 (d, *J* = 8.0 Hz, 1H), 6.17 (s, 1H), 5.86 (d, *J* = 8.5 Hz, 2H), 4.28 (dd, *J* = 11.2, 4.2 Hz, 1H), 4.06 (d, *J* = 17.4 Hz, 1H), 3.89 (d, *J* = 17.4 Hz, 1H), 3.80 (s, 3H), 3.73 (dd, *J* = 16.0, 4.3 Hz, 1H), 3.64 – 3.51 (m, 3H), 3.38 (dd, *J* = 13.9, 6.9 Hz, 1H), 3.20 (dd, *J* = 15.7, 11.7 Hz, 1H), 2.95 (s, 2H), 2.01 (s, 2H), 1.72 (s, 2H), 1.51 (dd, *J* = 13.7, 6.9 Hz, 2H), 1.36 (d, *J* = 20.3 Hz, 3H). HRMS (EI) *m/z* calcd for $C_{36}H_{38}N_4O_5$ (M^+) 606.2842, found 606.2844.

(6*R*,12a*R*)-6-(benzo[*d*][1,3]dioxol-5-yl)-2-(2-(1-(3-nitrobenzyl)piperidin-4-yl)ethyl)-2,3,6,7,12,12a-hexahydropyrazino[1',2':1,6]pyrido[3,4-*b*]indole-1,4-dione (2q). The electrophilic reagent was 3-nitrolbenzyl bromide. White solid, 53% yield, mp 124-126 °C. ^{1}H NMR (500 MHz, $CDCl_3$) δ 8.16 (d, *J* = 35.8 Hz, 2H), 7.86 (s, 1H), 7.60 (t, *J* = 45.3 Hz, 2H), 7.27 (s, 2H), 7.18 (s, 2H), 6.85 (s, 1H), 6.71 (d, *J* = 15.8 Hz, 1H), 6.18 (s, 1H), 5.87 (d, *J* = 11.2 Hz, 2H), 4.30 (s, 1H), 4.08 (d, *J* = 17.4 Hz, 1H),

3.92 (d, J = 17.1 Hz, 1H), 3.75 (d, J = 15.6 Hz, 1H), 3.68 – 3.31 (m, 4H), 3.31 – 3.12 (m, 1H), 2.84 (s, 2H), 1.97 (s, 2H), 1.73 (s, 2H), 1.59 (s, 2H), 1.26 (s, 3H). HRMS (EI) *m/z* calcd for $C_{35}H_{35}N_5O_6$ (M^+) 623.2699, found 623.2698.

Inhibition of ChE

The ChE assay was performed using the method of Ellman et al. with a slight modification[53]. The rat cortex was homogenized in cold 75 mM sodium phosphate buffer (pH 7.4) as the AChE source, and the rat serum was collected as the BuChE source. The assay solution consisted of 50 μL 0.1 M phosphate buffer, 50 μL 0.2% 5,5'-dithiobis (2-nitrobenzoic acid) (DTNB, Sigma), 109 μL or 99 μL deionized water, 10 μL rat cortex homogenate or 20 μL rat serum, and 30 μL 2 mM acetylthiocholine iodide (Sigma) or 40 μL 2 mM butyrylthiocholine (Sigma) as the substrate of the AChE or BuChE enzymatic reaction, respectively. An appropriate concentration of compound (1 nM-10 mM; 1 μL) and the assay solution were mixed and then incubated for 20 min at room temperature. The production of the yellow anion of 5-thio-2-nitrobenzoic acid was measured with a microplate reader (DTX 880, Beckman Coulter) at 450 nm. The inhibition percentage caused by the presence of test compound was calculated, and the IC_{50} was defined as the concentration of the compound that reduced 50% of the enzymatic activity without inhibitor.

Inhibition of PDE

The IMAP-FP assays were performed to measure the inhibitory activities of PDEs (PDE2A1, PDE3A, PDE4D3, PDE5A1, PDE6C, PDE7A and PDE9A2) by Shanghai ChemPartner Co. Ltd., in which binding of the hydrolyzed fluorescent cyclic nucleotide substrate to the IMAP reagent increases fluorescence polarization. Briefly, a 0.2-μL compound aliquot was transferred into a 384-well plate, and then 10 μL recombinant PDEs (BPS Biosciences) was added and incubated for 15 min at room temperature. Subsequently, 10 μL FAM-cAMP (for PDE2A1, PDE3A, PDE4D3, PDE7A) or FAM-cGMP (for PDE5A1, PDE6C, PDE9A2) was added to initiate the reaction. Reactions were incubated for 30 min (excluding 6 h for PDE6C)

at room temperature and were terminated by addition of IMAP binding reagent (Molecular Devices, Product No. R7287). The assay plate was placed in the dark and incubated for 1 h at room temperature. Fluorescence polarization intensity was measured at 485 nm excitation and 535 nm emission using a microplate reader (Victor3 V 1420 Multilabel Counter, Perkin Elmer). PDE inhibitors were dissolved in dimethyl sulfoxide (DMSO) at a final concentration of 1%. The inhibition percentage caused by the presence of test compound was calculated, and the IC_{50} was defined as the concentration of the compound that reduced 50% of the enzymatic activity without inhibitor.

In vitro Blood-Brain Barrier Permeation Assay

Brain penetration of compounds was evaluated using a parallel artificial membrane permeation assay (PAMPA) as described by Di *et al*.[56] The porcine brain lipid (PBL) was obtained from Avanti Polar Lipids. The donor microplate (PVDF membrane, pore size 0.45 mm) and the acceptor microplate were purchased from Millipore. The 96-well UV plate was from Corning Incorporated. The acceptor 96-well microplate was filled with 300 μL of PBS:EtOH (7:3, v:v), and the filter membrane was impregnated with 4 μL PBL in dodecane (20 mg mL^{-1}). Compounds were dissolved in DMSO at 5 mg mL^{-1} and diluted to 100 μg mL^{-1} with PBS:EtOH (7:3, v:v), and then 200 μL was added to the donor wells. The acceptor filter plate was carefully placed on the donor plate to form a sandwich, which was left undisturbed for 12 h at 25 °C. After incubation, the donor plate was carefully removed, and the concentration of compounds in the acceptor wells was determined using a UV plate reader (SpectraMax i3x). Each sample was analyzed at eight wavelengths in four wells in at least three independent runs, and the results are presented as the mean ± standard deviation. In the experiment, 13 quality control standards of known BBB permeability (Table S2, Supporting Information) were included to validate the analysis set. P_e was calculated using the following equation.

$$P_e = -\left(\frac{V_d \times V_a}{(V_d + V_a)\ A \times t}\right) \times \ln\left(1 - \frac{[drug]_{acceptor}}{[drug]_{equilibrium}}\right)$$

where V_d is the volume in the donor well, V_a is the volume in the acceptor well, A is the filter area, t is the permeation time, $[drug]_{acceptor}$ is the absorbance of the compound in the acceptor well, and $[drug]_{equilibrium}$ is the theoretical equilibrium absorbance.

Passageway Water Maze Test

Imprinting control region (ICR) mice (18–20 g) were obtained from the Shanghai Laboratory Animal Center, Chinese Academy of Sciences. The animal handling and experiment protocols were approved by the Institutional Animal Care and Use Committee of the Shanghai Institute of Materia Medica.

A passageway water maze (80 cm × 50 cm × 20 cm) was used to evaluate the cognition and memory of the mice. First, all mice were trained twice a day for 4 sequential days, and then the trained mice were randomly divided into five groups for the cognitive ability test: (1) control group (Ctrl), which was treated with solvent (p.o.) and saline (i.p.); (2) Scopolamine group (Scop), which was treated with solvent (p.o.) and scopolamine (4.5 mg/kg, i.p.); (3) Scop + donepezil group, which was treated with donepezil (10 mg/kg, p.o.) and scopolamine (4.5 mg/kg, i.p.); (4) Scop + 1p·Cit group, which was treated with 1p·Cit (10 mg/kg, p.o.) and scopolamine (4.5 mg/kg, i.p.); (5) Scop + 1w·Cit group, which was treated with 1w·Cit (10 mg/kg, p.o.) and scopolamine (4.5 mg/kg, i.p.). Next, the mice in each group were intragastrically administered the corresponding drug dosage in a 30% polyethylene glycol 400 (PEG400) solution. Forty minutes later, scopolamine (4.5 mg/kg) was injected (i.p.) in each group of mice except the control group, which was injected with saline. Twenty minutes later, the cognitive ability of the mice in each group was tested, by recording the escape latency and number of errors (entering no-exit paths).

Western Blot Analysis of Brain Samples

The mice were sacrificed after behavior tests, and the cortex was rapidly removed. The tissue samples were lysed in RIPA buffer (50 mM Tris-HCl, 150 mM NaCl, 0.5% sodium deoxycholate, 1% Triton X-100, 0.1% SDS, 1 mM NaF, 1 mM

Na_3VO_4,1 mM PMSF, 1% P8340, pH 7.4) for 30 min on ice and then centrifuged at 12000 × *g* for 15 min at 4 ℃. The supernatants were collected and mixed with loading buffer containing 5% DTT and boiled for 10 min. The proteins were separated using 10% sodium dodecyl sulfate-polyacrylamide gel electrophoresis and transferred onto nitrocellulose membranes. After blocking with 5% nonfat milk for 1 h at room temperature, the membranes were incubated with the following primary antibodies at 4 ℃ overnight: Phospho-CREB (Ser133) (Cell Signaling Technology), CREB (Cell Signaling Technology), β-actin (Sigma). HRP-conjugated secondary antibodies (1:5000, Kangchen Biotechnology) were incubated at room temperature for 1 h，and the bands were then visualized using an ECL kit (Millipore).

Statistical Analysis

Data were analyzed using an unpaired t test for comparison of two groups. A p value < 0.05 was considered to be significant.

Molecular Docking Studies

To perform the molecular docking, we analyzed the publicly available crystal structures as docking templates: hAChE complexed with donepezil (PDB ID 4EY7), and PDE5A complexed with tadalafil (PDB ID 2V60). The docking procedure was performed by employing the Surflex-dock implanted in TriposSybyl 2.0. During the process of docking, proteins were prepared, all water molecules were eliminated, the co-crystallized ligands were used to define the binding site, and CScore was chosen as the fitting function.

ASSOCIATED CONTENT

The Supporting Information is available free of charge on the ACS Publications website (http://pubs.acs.org).

HPLC reports for the purity check of compounds **1a-w** and **2a-q**, details of the synthetic procedures and structural characterizations of compounds **1p·Cit**, **1w·Cit** and intermediates **3a-d**, **4a-d** and **6-13**, data of calibration assay for BBB permeability

determination.

AUTHOR INFORMATION

Corresponding Authors

* For. J.L: phone, +86-21-64252584; fax, +86-21-64252584; Email, jianli@ecust.edu.cn; For H.Z: phone, +86-21-50806710; E-mail, hzhang@simm.ac.cn.

Author Contributions

#These authors contributed equally to this work.

Notes

The authors declare no competing financial interest.

ACKNOWLEDGMENTS

Financial support for this research provided by the National Key R&D Program of China (Grant 2017YFB0202600), the National Natural Science Foundation of China (Grant 21672064, 81522045), the Shanghai Sailing Program (Grants 17YF1403600), the "Shu Guang" project supported by the Shanghai Municipal Education Commission and Shanghai Education Development Foundation (Grant 14SG28), and the Fundamental Research Funds for the Central Universities are gratefully acknowledged.

ABBREVIATIONS USED

AChE, acetylcholinesterase; phosphodiesterase 5, PDE5; ChEs, cholinesterases; AD, alzheimer's disease; BBB, blood-brain barrier; MTDLs, multitarget-directed ligands; FDA, United States Food and Drug Administration; NMDAR, N-methyl-D-aspartate receptor; Hup A, huperzine A; CFDA, Chinese Food and Drug Administration; ACh, acetylcholine; Aβ, beta amyloid protein; MAO, monoamine oxidase; 5-HT_4R, serotonergic subtype 4 receptor; PDEs, phosphodiesterases; cAMP, cyclic adenosine

monophosphate; cGMP, cyclic guanosine monophosphate; CREB, cAMP response element-binding protein; LTP, long-term potentiation; CSF, cerebrospinal fluid; ED, erectile dysfunction; SAR, structure-activity relationship; BuChE, butyrylcholinesterase; IMAP-FP, immobilized metal ion affinity-based fluorescence polarization; Don, donepezil; Scop, scopolamine; DCM, dichloromethane; PAMPA, parallel artificial membrane permeation assay; DMSO, dimethyl sulfoxide

REFERENCES

(1) Blennow, K., de Leon, M. J., and Zetterberg, H. (2006) Alzheimer's disease. *Lancet 368*, 387-403.

(2) Shidore, M., Machhi, J., Shingala, K., Murumkar, P., Sharma, M. K., Agrawal, N., Tripathi, A., Parikh, Z., Pillai, P., and Yadav, M. R. (2016) Benzylpiperidine-Linked Diarylthiazoles as Potential Anti-Alzheimer's Agents: Synthesis and Biological Evaluation. *J. Med. Chem. 59*, 5823-5846.

(3) Bolea, I., Juárez-Jiménez, J., de los Ríos, C., Chioua, M., Pouplana, R., Luque, F. J., Unzeta, M., Marco-Contelles, J., and Samadi, A. (2011) Synthesis, Biological Evaluation, and Molecular Modeling of Donepezil and N-[(5-(Benzyloxy)-1-methyl-1H-indol-2-yl)methyl]-N-methylprop-2-yn-1-amine Hybrids as New Multipotent Cholinesterase/Monoamine Oxidase Inhibitors for the Treatment of Alzheimer's Disease. *J. Med. Chem. 54*, 8251-8270.

(4) Simoni, E., Daniele, S., Bottegoni, G., Pizzirani, D., Trincavelli, M. L., Goldoni, L., Tarozzo, G., Reggiani, A., Martini, C., Piomelli, D., Melchiorre, C., Rosini, M., and Cavalli, A. (2012) Combining galantamine and memantine in multitargeted, new chemical entities potentially useful in Alzheimer's disease. *J. Med. Chem. 55*, 9708-9721.

(5) Veloso, A. J., Chow, A. M., Dhar, D., Tang, D. W., Ganesh, H. V., Mikhaylichenko, S., Brown, I. R., and Kerman, K. (2013) Biological activity of sym-triazines with acetylcholine-like substitutions as multitarget modulators of Alzheimer's disease. *ACS Chem. Neurosci. 4*, 924-929.

(6) Sheng, R., Tang, L., Jiang, L., Hong, L., Shi, Y., Zhou, N., and Hu, Y. (2016)

Novel 1-Phenyl-3-hydroxy-4-pyridinone Derivatives as Multifunctional Agents for the Therapy of Alzheimer's Disease. *ACS Chem. Neurosci. 7*, 69-81.

(7) Wang, Z., Wang, Y., Wang, B., Li, W., Huang, L., and Li, X. (2015) Design, Synthesis, and Evaluation of Orally Available Clioquinol-Moracin M Hybrids as Multitarget-Directed Ligands for Cognitive Improvement in a Rat Model of Neurodegeneration in Alzheimer's Disease. *J. Med. Chem. 58*, 8616-8637.

(8) Liu, Y., Xie, Z., Zhao, D., Zhu, J., Mao, F., Tang, S., Xu, H., Luo, C., Geng, M., Huang, M., and Li, J. (2017) Development of the First Generation of Disulfide-Based Subtype-Selective and Potent Covalent Pyruvate Dehydrogenase Kinase 1 (PDK1) Inhibitors. *J. Med. Chem. 60*, 2227-2244.

(9) Liu, W., Rabinovich, A., Nash, Y., Frenkel, D., Wang, Y. Q., Youdim, M. B. H., and Weinreb, O. (2017) Anti-inflammatory and protective effects of MT-031, a novel multitarget MAO-A and AChE/BuChE inhibitor in scopolamine mouse model and inflammatory cells. *Neuropharmacology 113*, 445-456.

(10) Fernandez-Bachiller, M. I., Perez, C., Monjas, L., Rademann, J., and Rodriguez-Franco, M. I. (2012) New tacrine-4-oxo-4H-chromene hybrids as multifunctional agents for the treatment of Alzheimer's disease, with cholinergic, antioxidant, and beta-amyloid-reducing properties. *J. Med. Chem. 55*, 1303-1317.

(11) Panek, D., Wieckowska, A., Wichur, T., Bajda, M., Godyn, J., Jonczyk, J., Mika, K., Janockova, J., Soukup, O., Knez, D., Korabecny, J., Gobec, S., and Malawska, B. (2017) Design, synthesis and biological evaluation of new phthalimide and saccharin derivatives with alicyclic amines targeting cholinesterases, beta-secretase and amyloid beta aggregation. *Eur. J. Med. Chem. 125*, 676-695.

(12) Bhakta, H. K., Park, C. H., Yokozawa, T., Min, B. S., Jung, H. A., and Choi, J. S. (2016) Kinetics and molecular docking studies of loganin, morroniside and 7-O-galloyl-D-sedoheptulose derived from Corni fructus as cholinesterase and beta-secretase 1 inhibitors. *Arch. Pharmacal Res. 39*, 794-805.

(13) Nepovimova, E., Uliassi, E., Korabecny, J., Pena-Altamira, L. E., Samez, S., Pesaresi, A., Garcia, G. E., Bartolini, M., Andrisano, V., Bergamini, C., Fato, R.,

Lamba, D., Roberti, M., Kuca, K., Monti, B., and Bolognesi, M. L. (2014) Multitarget drug design strategy: quinone-tacrine hybrids designed to block amyloid-beta aggregation and to exert anticholinesterase and antioxidant effects. *J. Med. Chem. 57*, 8576-8589.

(14) Kochi, A., Eckroat, T. J., Green, K. D., Mayhoub, A. S., Lim, M. H., and Garneau-Tsodikova, S. (2013) A novel hybrid of 6-chlorotacrine and metal-amyloid-β modulator for inhibition of acetylcholinesterase and metal-induced amyloid-β aggregation. *Chem. Sci. 4*, 4137-4145.

(15) Veloso, A. J., Dhar, D., Chow, A. M., Zhang, B., Tang, D. W. F., Ganesh, H. V. S., Mikhaylichenko, S., Brown, I. R., and Kerman, K. (2013) sym-Triazines for Directed Multitarget Modulation of Cholinesterases and Amyloid-β in Alzheimer's Disease. *ACS Chem. Neurosci. 4*, 339-349.

(16) Yanez, M., and Vina, D. (2013) Dual Inhibitors of Monoamine Oxidase and Cholinesterase for the Treatment of Alzheimer Disease. *Curr. Top. Med. Chem. 13*, 1692-1706.

(17) Bautista-Aguilera, O. M., Esteban, G., Chioua, M., Nikolic, K., Agbaba, D., Moraleda, I., Iriepa, I., Soriano, E., Samadi, A., Unzeta, M., and Marco-Contelles, J. (2014) Multipotent cholinesterase/monoamine oxidase inhibitors for the treatment of Alzheimer's disease: design, synthesis, biochemical evaluation, ADMET, molecular modeling, and QSAR analysis of novel donepezil-pyridyl hybrids. *Drug Des. Dev. Ther. 8*, 1893-1910.

(18) Rochais, C., Lecoutey, C., Gaven, F., Giannoni, P., Hamidouche, K., Hedou, D., Dubost, E., Genest, D., Yahiaoui, S., Freret, T., Bouet, V., Dauphin, F., Sopkova de Oliveira Santos, J., Ballandonne, C., Corvaisier, S., Malzert-Freon, A., Legay, R., Boulouard, M., Claeysen, S., and Dallemagne, P. (2015) Novel multitarget-directed ligands (MTDLs) with acetylcholinesterase (AChE) inhibitory and serotonergic subtype 4 receptor (5-HT4R) agonist activities as potential agents against Alzheimer's disease: the design of donecopride. *J. Med. Chem. 58*, 3172-3187.

(19) Nepovimova, E., Korabecny, J., Dolezal, R., Babkova, K., Ondrejicek, A., Jun, D., Sepsova, V., Horova, A., Hrabinova, M., Soukup, O., Bukum, N., Jost, P., Muckova, L., Kassa, J., Malinak, D., Andrs, M., and Kuca, K. (2015) Tacrine-Trolox Hybrids: A Novel Class of Centrally Active, Nonhepatotoxic Multi-Target-Directed Ligands Exerting Anticholinesterase and Antioxidant Activities with Low In Vivo Toxicity. *J. Med. Chem. 58*, 8985-9003.

(20) Fernandez-Bachiller, M. I., Perez, C., Campillo, N. E., Paez, J. A., Gonzalez-Munoz, G. C., Usan, P., Garcia-Palomero, E., Lopez, M. G., Villarroya, M., Garcia, A. G., Martinez, A., and Rodriguez-Franco, M. I. (2009) Tacrine-Melatonin Hybrids as Multifunctional Agents for Alzheimer's Disease, with Cholinergic, Antioxidant, and Neuroprotective Properties. *ChemMedChem 4*, 828-841.

(21) Zheng, H., Youdim, M. B. H., and Fridkin, M. (2009) Site-Activated Multifunctional Chelator with Acetylcholinesterase and Neuroprotective−Neurorestorative Moieties for Alzheimer's Therapy. *J. Med. Chem. 52*, 4095-4098.

(22) Joubert, J., Foka, G. B., Repsold, B. P., Oliver, D. W., Kapp, E., and Malan, S. F. (2017) Synthesis and evaluation of 7-substituted coumarin derivatives as multimodal monoamine oxidase-B and cholinesterase inhibitors for the treatment of Alzheimer's disease. *Eur. J. Med. Chem. 125*, 853-864.

(23) Domek-Lopacinska, K. U., and Strosznajder, J. B. (2010) Cyclic GMP and Nitric Oxide Synthase in Aging and Alzheimer's Disease. *Mol. Neurobiol. 41*, 129-137.

(24) Francis, S. H., Blount, M. A., and Corbin, J. D. (2011) Mammalian cyclic nucleotide phosphodiesterases: molecular mechanisms and physiological functions. *Physiol. Rev. 91*, 651-690.

(25) Yin, J. C., and Tully, T. (1996) CREB and the formation of long-term memory. *Curr. Opin. Neurobiol. 6*, 264-268.

(26) Tully, T. (1997) Regulation of gene expression and its role in long-term memory and synaptic plasticity. *Proc. Natl. Acad. Sci. U. S. A. 94*, 4239-4241.

(27) Reneerkens, O. A. H., Rutten, K., Steinbusch, H. W. M., Blokland, A., and Prickaerts, J. (2009) Selective phosphodiesterase inhibitors: a promising target for cognition enhancement. *Psychopharmacology 202*, 419-443.

(28) Jin, F., Gong, Q. H., Xu, Y. S., Wang, L. N., Jin, H., Li, F., Li, L. S., Ma, Y. M., and Shi, J. S. (2014) Icariin, a phosphodiesterase-5 inhibitor, improves learning and memory in APP/PS1 transgenic mice by stimulation of NO/cGMP signalling. *Int. J. Neuropsychopharmacol. 17*, 871-881.

(29) Zhu, L., Yang, J. Y., Xue, X., Dong, Y. X., Liu, Y., Miao, F. R., Wang, Y. F., Xue, H., and Wu, C. F. (2015) A novel phosphodiesterase-5 Inhibitor: Yonkenafil modulates neurogenesis, gliosis to improve cognitive function and ameliorates amyloid burden in an APP/PS1 transgenic mice model. *Mech. Ageing Dev. 150*, 34-45.

(30) Gomez, L., Massari, M. E., Vickers, T., Freestone, G., Vernier, W., Ly, K., Xu, R., McCarrick, M., Marrone, T., Metz, M., Yan, Y. G., Yoder, Z. W., Lemus, R., Broadbent, N. J., Barido, R., Warren, N., Schmelzer, K., Neul, D., Lee, D., Andersen, C. B., Sebring, K., Aertgeerts, K., Zhou, X., Tabatabaei, A., Peters, M., and Breitenbucher, J. G. (2017) Design and Synthesis of Novel and Selective Phosphodiesterase 2 (PDE2a) Inhibitors for the Treatment of Memory Disorders. *J. Med. Chem. 60*, 2037-2051.

(31) Park, S. H., Kim, J. H., Bae, S. S., Hong, K. W., Lee, D. S., Leem, J. Y., Choi, B. T., and Shin, H. K. (2011) Protective effect of the phosphodiesterase III inhibitor cilostazol on amyloid beta-induced cognitive deficits associated with decreased amyloid beta accumulation. *Biochem. Biophys. Res. Commun. 408*, 602-608.

(32) Sakurai, H., Hanyu, H., Sato, T., Kume, K., Hirao, K., Kanetaka, H., and Iwamoto, T. (2013) Effects of cilostazol on cognition and regional cerebral blood flow in patients with Alzheimer's disease and cerebrovascular disease: a pilot study. *Geriatr. Gerontol. Int. 13*, 90-97.

(33) Gong, B., Vitolo, O. V., Trinchese, F., Liu, S., Shelanski, M., and Arancio, O. (2004) Persistent improvement in synaptic and cognitive functions in an Alzheimer mouse model after rolipram treatment. *J. Clin. Invest. 114*, 1624-1634.

(34) Li, J., Liu, C. N., Wei, N., Li, X. D., Liu, Y. Y., Yang, R., and Jia, Y. J. (2016) Protective effects of BAY 73-6691, a selective inhibitor of phosphodiesterase 9, on amyloid-β peptides-induced oxidative stress in in-vivo and in-vitro models of Alzheimer's disease. *Brain Res. 1642*, 327-335.

(35) García-Osta, A., Cuadrado-Tejedor, M., García-Barroso, C., Oyarzábal, J., and Franco, R. (2012) Phosphodiesterases as Therapeutic Targets for Alzheimer's Disease. *ACS Chem. Neurosci. 3*, 832-844.

(36) Sánchez-Arias, J. A., Rabal, O., Cuadrado-Tejedor, M., de Miguel, I., Pérez-González, M., Ugarte, A., Sáez, E., Espelosin, M., Ursua, S., Haizhong, T., Wei, W., Musheng, X., Garcia-Osta, A., and Oyarzabal, J. (2017) Impact of Scaffold Exploration on Novel Dual-Acting Histone Deacetylases and Phosphodiesterase 5 Inhibitors for the Treatment of Alzheimer's Disease. *ACS Chem. Neurosci. 8*, 638-661.

(37) Heckman, P. R. A., Blokland, A., Ramaekers, J., and Prickaerts, J. (2015) PDE and cognitive processing: Beyond the memory domain. *Neurobiol. Learn. Mem. 119*, 108-122.

(38) Ugarte, A., Gil-Bea, F., Garcia-Barroso, C., Cedazo-Minguez, A., Ramirez, M. J., Franco, R., Garcia-Osta, A., Oyarzabal, J., and Cuadrado-Tejedor, M. (2015) Decreased levels of guanosine 3', 5'-monophosphate (cGMP) in cerebrospinal fluid (CSF) are associated with cognitive decline and amyloid pathology in Alzheimer's disease. *Neuropathol. Appl. Neurobiol. 41*, 471-482.

(39) Cuadrado-Tejedor, M., Hervias, I., Ricobaraza, A., Puerta, E., Perez-Roldan, J. M., Garcia-Barroso, C., Franco, R., Aguirre, N., and Garcia-Osta, A. (2011) Sildenafil restores cognitive function without affecting beta-amyloid burden in a mouse model of Alzheimer's disease. *Br. J. Pharmacol. 164*, 2029-2041.

(40) Garcia-Barroso, C., Ricobaraza, A., Pascual-Lucas, M., Unceta, N., Rico, A. J., Goicolea, M. A., Salles, J., Lanciego, J. L., Oyarzabal, J., Franco, R., Cuadrado-Tejedor, M., and Garcia-Osta, A. (2013) Tadalafil crosses the blood-brain barrier and reverses cognitive dysfunction in a mouse model of AD. *Neuropharmacology 64*, 114-123.

(41) Prickaerts, J., Sik, A., van der Staay, F. J., de Vente, J., and Blokland, A. (2005) Dissociable effects of acetylcholinesterase inhibitors and phosphodiesterase type 5 inhibitors on object recognition memory: acquisition versus consolidation. *Psychopharmacology 177*, 381-390.

(42) Chong, C. R., and Sullivan, D. J. (2007) New uses for old drugs. *Nature 448*, 645-646.

(43) Liu, Y. F., Xie, Z. Q., Zhao, D., Zhu, J., Mao, F., Tang, S., Xu, H., Luo, C., Geng, M. Y., Huang, M., and Li, J. (2017) Development of the First Generation of Disulfide-Based Subtype Selective and Potent Covalent Pyruvate Dehydrogenase Kinase 1 (PDK1) Inhibitors. *J. Med. Chem. 60*, 2227-2244.

(44) Sun, W. Y., Xie, Z. Q., Liu, Y. F., Zhao, D., Wu, Z. X., Zhang, D. D., Lv, H., Tang, S., Jin, N., Jiang, H. L., Tan, M. J., Ding, J., Luo, C., Li, J., Huang, M., and Geng, M. Y. (2015) JX06 Selectively Inhibits Pyruvate Dehydrogenase Kinase PDK1 by a Covalent Cysteine Modification. *Cancer Res. 75*, 4923-4936.

(45) Chen, F. F., Di, H. X., Wang, Y. X., Cao, Q., Xu, B., Zhang, X., Yang, N., Liu, G. J., Yang, C. G., Xu, Y., Jiang, H. L., Lian, F. L., Zhang, N. X., Li, J., and Lan, L. F. (2016) Small-molecule targeting of a diapophytoene desaturase inhibits S. aureus virulence. *Nat. Chem. Biol. 12*, 174-179.

(46) Wang, Y., Di, H., Chen, F., Xu, Y., Xiao, Q., Wang, X., Wei, H., Lu, Y., Zhang, L., Zhu, J., Lan, L., and Li, J. (2016) Discovery of Benzocycloalkane Derivatives Efficiently Blocking Bacterial Virulence for the Treatment of Methicillin-Resistant S. aureus (MRSA) Infections by Targeting Diapophytoene Desaturase (CrtN). *J. Med. Chem. 59*, 4831-4848.

(47) Wang, Y., Chen, F., Di, H., Xu, Y., Xiao, Q., Wang, X., Wei, H., Lu, Y., Zhang, L., Zhu, J., Sheng, C., Lan, L., and Li, J. (2016) Discovery of Potent Benzofuran-Derived Diapophytoene Desaturase (CrtN) Inhibitors with Enhanced Oral Bioavailability for the Treatment of Methicillin-Resistant Staphylococcus aureus (MRSA) Infections. *J. Med. Chem. 59*, 3215-3230.

(48) Kulkarni, S. K., and Patil, C. S. (2004) Phosphodiesterase 5 enzyme and its inhibitors: update on pharmacological and therapeutical aspects. *Methods Find. Exp. Clin. Pharmacol. 26*, 789-799.

(49) Forgue, S. T., Patterson, B. E., Bedding, A. W., Payne, C. D., Phillips, D. L., Wrishko, R. E., and Mitchell, M. I. (2006) Tadalafil pharmacokinetics in healthy subjects. *Br. J. Clin. Pharmacol. 61*, 280-288.

(50) Daugan, A., Grondin, P., Ruault, C., Le Monnier de Gouville, A. C., Coste, H., Kirilovsky, J., Hyafil, F., and Labaudiniere, R. (2003) The discovery of tadalafil: a novel and highly selective PDE5 inhibitor. 1: 5,6,11,11a-tetrahydro-1H-imidazo[1',5':1,6]pyrido[3,4-b]indole-1,3(2H)-dione analogues. *J. Med. Chem. 46*, 4525-4532.

(51) Daugan, A., Grondin, P., Ruault, C., Le Monnier de Gouville, A. C., Coste, H., Linget, J. M., Kirilovsky, J., Hyafil, F., and Labaudiniere, R. (2003) The discovery of tadalafil: a novel and highly selective PDE5 inhibitor. 2: 2,3,6,7,12,12a-hexahydropyrazino[1',2':1,6]pyrido[3,4-b]indole-1,4-dione analogues. *J. Med. Chem.46*, 4533-4542.

(52) Aldrich, C., Bertozzi, C., Georg, G. I., Kiessling, L., Lindsley, C., Liotta, D., Merz, K. M., Jr., Schepartz, A., and Wang, S. (2017) The Ecstasy and Agony of Assay Interference Compounds. *ACS Med. Chem. Lett. 8*, 379-382.

(53) Ellman, G. L., Courtney, K. D., Andres, V., Jr., and Feather-Stone, R. M. (1961) A new and rapid colorimetric determination of acetylcholinesterase activity. *Biochem. Pharmacol. 7*, 88-95.

(54) Sportsman, J. R., Gaudet, E. A., and Boge, A. (2004) Immobilized metal ion affinity-based fluorescence polarization (IMAP): advances in kinase screening. *Assay Drug Dev. Technol. 2*, 205-214.

(55) Nunes, I. K., de Souza, E. T., Cardozo, S. V., Carvalho, V. F., Romeiro, N. C., Silva, P. M., Martins, M. A., Barreiro, E. J., and Lima, L. M. (2016) Synthesis, Pharmacological Profile and Docking Studies of New Sulfonamides Designed as Phosphodiesterase-4 Inhibitors. *PloS one 11*, e0162895.

(56) Di, L., Kerns, E. H., Fan, K., McConnell, O. J., and Carter, G. T. (2003) High throughput artificial membrane permeability assay for blood-brain barrier. *Eur. J. Med. Chem. 38*, 223-232.

(57) Klinkenberg, I., and Blokland, A. (2010) The validity of scopolamine as a pharmacological model for cognitive impairment: a review of animal behavioral studies. *Neurosci. Biobehav. Rev. 34*, 1307-1350.

(58) Cheung, J., Rudolph, M. J., Burshteyn, F., Cassidy, M. S., Gary, E. N., Love, J., Franklin, M. C., and Height, J. J. (2012) Structures of human acetylcholinesterase in complex with pharmacologically important ligands. *J. Med. Chem. 55*, 10282-10286.

(59) Card, G. L., England, B. P., Suzuki, Y., Fong, D., Powell, B., Lee, B., Luu, C., Tabrizizad, M., Gillette, S., Ibrahim, P. N., Artis, D. R., Bollag, G., Milburn, M. V., Kim, S. H., Schlessinger, J., and Zhang, K. Y. (2004) Structural basis for the activity of drugs that inhibit phosphodiesterases. *Structure 12*, 2233-2247.

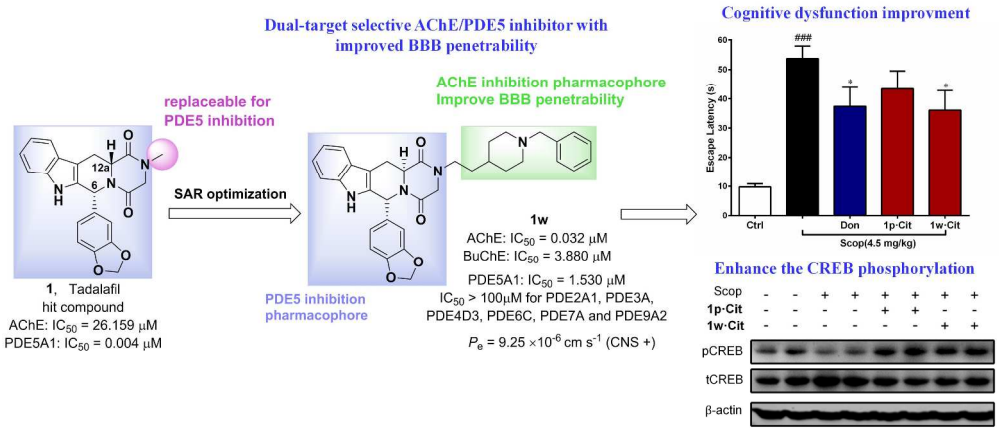

Table of Contents graphic

295x130mm (300 x 300 DPI)